Journal of Applied Polymer Science

WILEY

Applied Polymer SCIENCE

RESEARCH ARTICLE OPEN ACCESS

Thermo-Mechanical Degradation Kinetics of a High-Density Poly(Ethylene) Using a Closed-Cavity Rheometer

Tim Schülein[1,2] | Christos K. Georgantopoulos[1] | Lars Bolk[3] | Volker Herrmann[2] | Manfred Wilhelm[1]

[1]Institute for Chemical Technology and Polymer Chemistry, Karlsruhe Institute of Technology (KIT), Karlsruhe, Germany | [2]Technology Transfer Centre Haßfurt, Technical University of Applied Sciences Würzburg-Schweinfurt (THWS), Haßfurt, Germany | [3]Department of Chemistry, University of Konstanz, Konstanz, Germany

Correspondence: Manfred Wilhelm (manfred.wilhelm@kit.edu)

Received: 26 November 2024 | **Revised:** 23 December 2024 | **Accepted:** 2 January 2025

Funding: The authors received no specific funding for this work.

Keywords: degradation | kinetics | polyolefins | rheology | thermo-mechanical treatment

ABSTRACT

Mechanical recycling of polymers is an essential aspect to achieve circular economy. High shear stress, excessive temperature, and long residence time during reprocessing cause thermo-mechanical degradation of the polymer. Therefore, it is important to understand and quantify this degradation kinetics. Common ways to simulate degradation are very time and material consuming and clear insights into the respective influence of temperature and shear stress on degradation are rare. Within this publication a method is developed using a commercially available, close-cavity rheometer to emulate processing conditions in a defined way. This allows monitoring and predicting the behavior of a high-density polyethylene (HDPE) and quantify degradation kinetics and changes in the polymer topology. HDPE is selected as a model polymer due to its large production and wide range of applications. Different treated samples are analyzed by various rheological methods. Additionally, molecular characterization is conducted. A kinetic model to predict the changes in the molecular weight as a function of in-phase shear stress, temperature and duration during treatment is presented. The calculated activation energy for the initiation reaction agrees with the activation energy for HDPE degradation from thermogravimetric analysis. This activation energy is lowered by in-phase shear stress, modified by a factor of 1.7 $m^3 mol^{-1}$.

1 | Introduction

In order to promote sustainability and to reduce the consumption of fossil fuels it is important to develop further insights towards a circular economy of polymer materials [1]. Mechanical recycling is one of the most efficient ways to achieve this, but it involves multiple melting and reprocessing of the polymer material. The reprocessing can degrade the polymer both thermally and mechanically and consequently might cause poor solid mechanical properties during multiple usage. The thermo-mechanical degradation of the polymer is caused by the high processing temperatures ($T = 170°C–300°C$ for high-density polyethylene, HDPE) [2–4], high shear stress (approximately 10–100 kPa) [5], and long residence times during processing (up to 5 min) [2, 6] in an extruder.

Known mechanisms of polyolefin degradation are shown in Figure 1. First, macroradicals form due to thermo-mechanical treatment, leading to abstraction of protons [7–10]. It is also known that these macroradicals arise from temperature induced H-abstraction [11, 12]. These radicals can cause chain scission or chain branching [13]. Several studies consider that only the type of monomer and therefore the substituent —X (—H, —CH_3) on the polymer chain is responsible for the dominant reaction during degradation, for example for poly(ethylene) (PE) branching is predominantly observed, whereas poly(propylene) (PP)

predominantly displays chain scission [13]. However, other studies found that the reaction rate of the branching of polyethylene also depends on the concentration of unsaturated groups on the polymer (e.g., vinyl groups), which are still present after polymerization [6, 14]. This unintended functional groups in HDPE depend, for example, on the catalyst used [6, 15, 16].

It is common in the literature to investigate these phenomena via multiple extrusion of the material in a circular process to emulate the multiple processing steps and their influence on melt and solid polymer properties. This was shown by studies of different PE variants, for example, high-density polyethylene, HDPE [2–4, 6, 15, 17–21], low-density polyethylene, LDPE [4, 7, 21–23], and linear low-density polyethylene, LLDPE [14, 24]. Oblak et al. investigated the reprocessing of HDPE over 100 cycles [17] and found a strong reduction (−51%) of the weight-average molecular weight (Table 1) using high-temperature size exclusion chromatography (HT-SEC). This approach requires a lot of time and material to emulate the reprocessing, especially if the processing parameters are varied. One common way to solve this problem is to use an internal mixer [25, 26] or a continuously working extruder [27]. Doing so it is difficult to make clear predictions on the influence of the different parameters, for example, temperature, residence time, shear stress, and so forth, in an extruder. Specifically, the effect of the shear stress and the residence time is difficult to quantify because of a complex flow behavior within the extruder barrel. Therefore, only average values can be given using assumptions and simplifications for the extrusion process.

To avoid the complexity of the flow field within an extruder, a device is needed that applies a defined type of flow and specific, practically relevant shear rates (i.e., $\dot{\gamma} = 1–100\,s^{-1}$) at a fixed and defined temperature (i.e., $T = 170°C–300°C$). Custom-built devices, which are used to apply high shear stress, can also be found in literature [28, 29]. Additionally, commercially available rheometers have been used to apply thermo-mechanical treatment to different polymers [30–34]. Tikhomirov et al. used a standard Mooney viscometer to study the degradation reactions of styrene-butadiene rubber (SBR, unknown M_w and $Đ$) under a fixed shear stress (up to 114 arbitrary Mooney units) and temperature range ($T = 100°C–120°C$) [30]. Kaneyasu et al. used an open oscillatory shear (cone-plate) rheometer for degradation of a HDPE ($M_w = 157\,kg\,mol^{-1}$, $Đ = 5.7$). This has the advantage that changes in elastic and viscous modulus G' and G'', respectively, during degradation can be studied and quantified online. The authors used shear rates up to $\dot{\gamma} = 100\,s^{-1}$ at a temperature of $T = 180°C$ for $t = 10\,min$. They did not observe any detectable

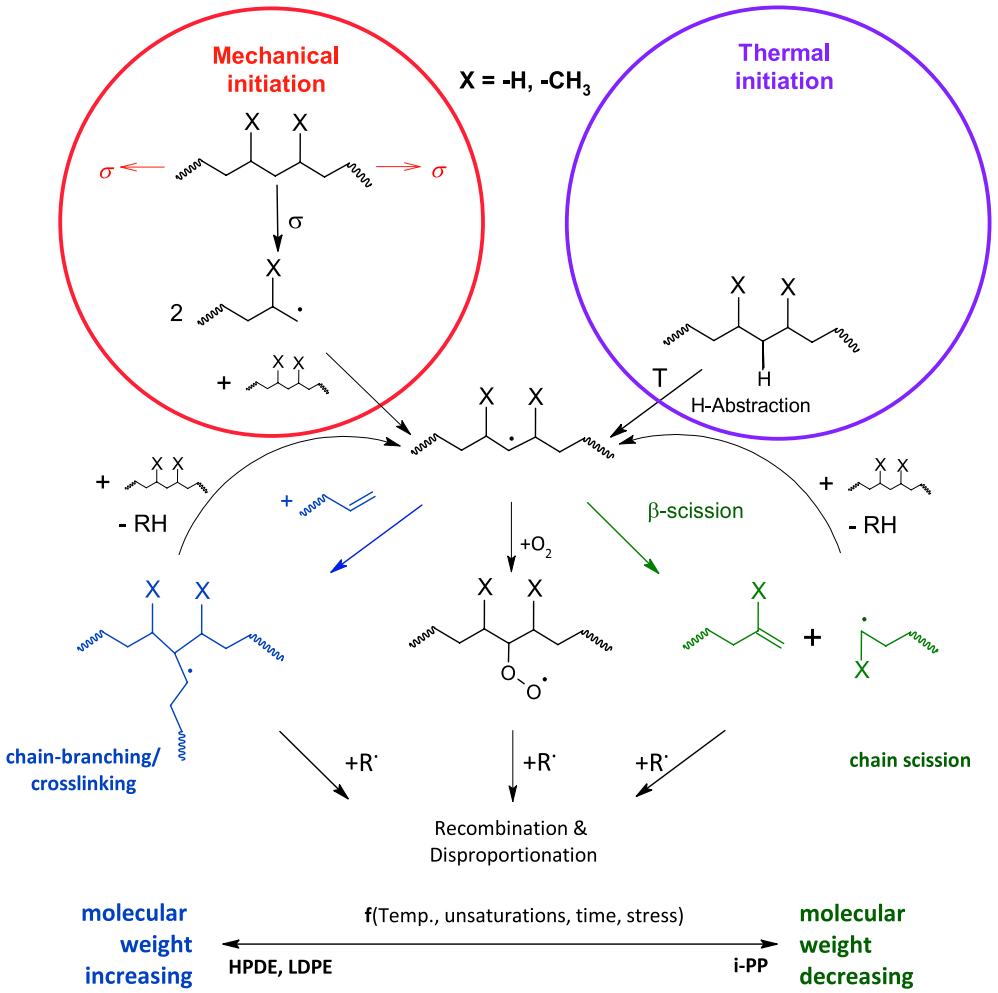

FIGURE 1 | Schematic overview of the thermo-mechanical degradation reactions of polyolefins and the resulting polymeric products. The predominant reaction pathway depends on the concentration of unsaturation, temperature, mechanical stress, and the duration of thermo-mechanical treatment. [Color figure can be viewed at wileyonlinelibrary.com]

TABLE 1 | Changes in molecular weight of the HDPE during extrusion as reported in literature.

Authors	T_{melt} (°C)	Type of extruder	Processing duration (min)	Change in M_w (%)	Stabilizer	Lit. reference
Langwieser et al.	220	Single screw	18[a]	+/−0	Processing and AO	[4]
Pinheiro et al.	240	Twin screw (co-rotating)	7.5	+17	None	[25]
Pinheiro et al.	240	Internal mixer	60	+21	None	[6]
Oblak et al.	240	Twin screw (co-rotating)	300[a]	−51	UV	[17]
Schweighuber et al.	220	Twin screw	120	−92	None	[27]
Moss et al.	240	Single screw	15[a]	+17	None	[16]

Note: Column "stabilizer" gives information about the polymer antioxidants (AO), UV-stabilizers (UV), and processing stabilizers (processing) used.
[a]Estimated from given parameters within the article.

TABLE 2 | Molecular characterization of the studied HDPE.

Material	M_w (kg mol^{-1})	$Đ$ (-)	$T_{m,peak}$ (°C)	Crystallinity[a] (%)	$\lvert\eta^*\rvert_0$ at 180°C (Pa s)	ρ at 25°C (g cm^{-3})	MFI (190°C, 2.16 kg) (g [10 min^{-1}])
HDPE	113.2	9.8	132.0	66.4	9.6×10^4	0.950	0.25

[a]Using a melting enthalpy for 100% crystalline PE of 293 J g^{-1}.

change in the structure of the polymer via the rheological and SEC data [31]. The group of Münstedt [32–34] used a different approach to determine the thermal stability of different polyethylene. They conducted time sweeps in an oscillatory rheometer over extended duration (up to $t = 28$ h) at different temperatures ($T = 130$°C–190°C) in nitrogen atmosphere and determined a change in the storage modulus G' (normalized change < 5% for 10^6 s for LDPE) for these polyethylene polymers [32–34]. They used only low angular frequencies (up to $\omega = 0.32$ rad s^{-1}) in the linear viscoelastic (LVE) regime, and thus did not study the mechanical influence on degradation, but they tested only thermal degradation.

The focus of this publication is on the method development using a closed-cavity rheometer for studying the thermo-mechanical degradation kinetics of polymer melts. Closed-cavity rheometers (CCR) can apply defined shear rates and high shear strains at defined temperature similar to extrusion for a defined time. Furthermore, this set-up prevents wall slippage and edge fracture for low viscous polymers due to their grooved plates and closed cavity, even at high shear strains, temperature and pressure [35]. The influence of oxygen is limited due to the sealing. Within this study, a CCR (Scarabaeus SIS V50, TA Instruments) was used to apply thermo-mechanical treatment using high shear strains ($\gamma_0 = 27\%–460\%$) at typical processing temperatures ($T = 160$°C–220°C) to quantify the time evolution on the HDPE sample. This specific HDPE was selected due to its wide range of usage, large production and presence in potentially recycled polyethylene. This article explores the use of this specific set up to study thermo-mechanical degradation applied via a CCR to quantify degradation kinetics.

2 | Materials and Methods

2.1 | Materials and Preparation

The investigated material is a commercially available unimodal HDPE with a broad molecular weight distribution (Table 2). It was polymerized using a Philips catalyst and is typically processed by blow molding, for products like packaging and engineering goods. This HDPE was chosen due to its wide range of applications and final solid mechanical properties. As a commercial product it contains 0.1%–0.5% of antioxidants. A polyethylene without antioxidants was not chosen because this would not reflect any practical use like mechanical recycling.

The test specimens are prepared by pressing the HDPE at $T = 200$°C and $p = 20$ MPa for $t = 5$ min and then punching out a disk (weight of the specimen $m = 2.5$ g). The temperature $T = 200$°C was chosen to ensure fast relaxation of the polymer chains during the pressing.

2.2 | Thermo-Mechanical Treatment and Rheological Measurements

The measurements were conducted using a closed-cavity rheometer (CCR, Scarabaeus, Model SIS V50), an oscillatory rheometer with biconical, grooved plates, and a sealed cavity, which prevents wall slippage and edge fracturing [35]. Hence, high shear strains up to $\gamma_0 = 460\%$ at $\omega/2\pi = 1$ Hz can be reached. This geometry is important to emulate the high shear stress during

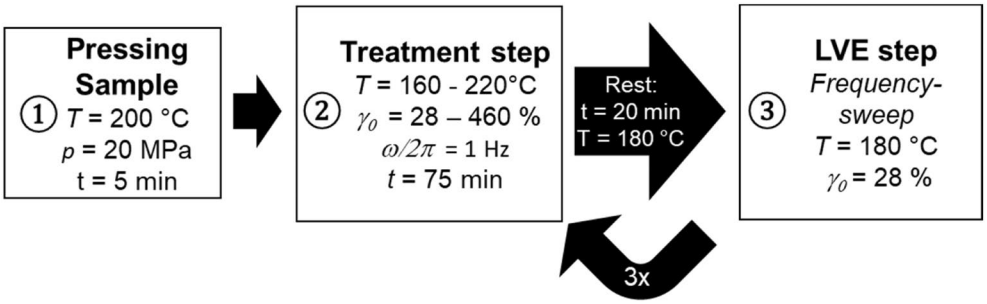

FIGURE 2 | Procedure to study thermo-mechanical treatment applying a closed-cavity rheometer (CCR). Pressed samples were subjected to a thermo-mechanical treatment during four treatment steps. Parameters are based on the data sheet, practical relevance, and the framework provided by the CCR. Rheological changes due to this treatment are subsequently analyzed in the LVE regime. A rest of 20 min between the treatment step and LVE analysis ensures relaxation of the polymer.

processing. The rheometer's temperature limit is $T = 220°C$ and shear rates up to $\dot{\gamma} = 80\,s^{-1}$ can be carried out.

The procedure of the thermo-mechanical treatment is shown in Figure 2. The treatment lasts 75 min in the closed geometry and is followed by a rest of 20 min in the still closed geometry at $T = 180°C$. The resting time provides relaxation of the molecules to reduce any effect of the high shear strains (i.e., memory effects) on the LVE-measurement [36]. It will be shown later, that there is no significant change in molecular weight during this rest. Afterwards, a measurement in the linear viscoelastic regime (LVE) is conducted to determine the rheological properties. This procedure is then repeated three more times to ensure a total treatment time of $4 \times 75\,min = 300\,min$. This time duration is chosen as an equivalent of about 60–100 reprocessing events within the extruder each with a typical residence time of about $t = 3$–$5\,min$ (see Figure 2). The temperature conditions are chosen to be within the recommended processing range, according to the material data sheet. The shear strain is varied to cause mechanically induced chemical change of the polymer chain. A frequency of $\omega/2\pi = 1\,Hz$ is chosen as a compromise between high shear stress and the online detection of rheological change. According to Debbaut and Burhin, the shear field inside the cavity is homogeneous [37]. All steps were conducted at an internal pressure of $p = 1\,MPa$ on the sample [38] within the CCR. This pressure is much less compared with pressures prevail during extrusion (range of tens MPa). Therefore, the influence of pressure on thermo-mechanical treatment (e.g., influence of pressure on degradation) cannot be evaluated within this setup.

To compare the various conditions during the treatment, the in-phase shear stress σ'_{treat} of the strain-controlled rheometer was studied, as it represents the shear stress stored and acting on the polymer chain. The stored shear stress was calculated from γ_0 and from treatment parameter resulting G':

$$\sigma'_{treat}(T, t, \gamma_0) = G'_{treat}(T, t) * \gamma_{0,treat} \tag{1}$$

This analysis was conducted at different samples at temperatures T_{treat} of 160°C, 180°C, 195°C, 210°C, and 220°C, all at a shear strain $\gamma_{0,treat}$ of 28%, 70%, 153%, 370%, and 460%. A new specimen was used for each set of conditions of T_{treat} and σ'_{treat}. Elongation rheology experiments were conducted at 150°C for the virgin and treated HDPE-samples using the extensional viscosity fixture (EVF) at an ARES G2 both from TA instruments. The Hencky rates were varied between $\dot{\epsilon} = 0.1$ and $10\,s^{-1}$.

To investigate the impact of temperature and shear stress during real life extrusion on the same material, the studied HDPE was extruded with a laboratory single screw extruder (Bernhard IDE GmbH & Co KG), specifically an IDE ME 45/5 extruder with a screw diameter of 30 mm, channel depth of 1.9 mm and standard three zones screw with a length of 900 mm. The temperature profile along the extruder was 160°C–200°C from the feed zone to die exit at a rotational rate of $n = 80\,rpm$. The residence time distribution and the temperature profile result in an average melt temperature of 190°C during the experiments. The used round die has a length of 10 mm and a diameter of 2 mm. The average resident time was measured by a colored tracing particle and found out to be around 3.5 min. The extruded HDPE was back fed to the extruder 9 times, so 10 extrusions in total. This resulted in a total resident time of around 35 min. The extruded HDPE was studied by HT-SEC and rheology and was compared with the above-mentioned treatment, see below. To estimate the shear stress during extrusion the following equation was used according to: [39]

$$\sigma_{extrusion} = \dot{\gamma} * \eta(\dot{\gamma}) = \frac{\pi D N}{H}\,\eta(\dot{\gamma}) \tag{2}$$

where D is the screw diameter in mm, H the channel depth in mm, and N the rotational speed in s^{-1}.

2.3 | High-Temperature Size Exclusion Chromatography

The molecular weight distribution (MWD) before and after the described thermo-mechanical treatment was investigated by means of a high-temperature size exclusion chromatography (HT-SEC). A sample was cut out of the edge of the degraded sample. It is shown in the results, that there is no significant oxidation even at the edge of the sample. The sample was dissolved in 1,2-dichlorobenzene to reach a concentration of $0.5\,g\,L^{-1}$. About 200 µL of this solution was injected and analyzed at a flow rate of $2\,mL\,min^{-1}$ and at a temperature of 160°C. The polymer was analyzed with an infra-red (IR) detector, which was calibrated with linear PE standard. The used IR-detector measured absorption of the CH_2-groups at $2920\,cm^{-1}$.

2.4 | Fourier-Transform Infrared Spectroscopy

Fourier-transform infrared spectroscopy (FTIR) is used to investigate degradation of the polyethylene by monitoring the change in the vinyl and carbonyl functional groups. The samples were cut out of the edge of the treated samples and films were pressed at 150°C and 110 bar for 5 min and then cooled with 10 K min^{-1}, resulting in a measured thickness of the film of $d = 70\,\mu m$. The analysis was carried out in transmission at room temperature using a Bruker Vertex 70 with a DTGS detector. The applied spectral resolution in the IR spectra was 2 cm^{-1}. The influence of data scattering is reduced by similar sample preparation and the use of spectral baseline correction [40]. Details of the baseline correction are described in the literature mentioned below.

Although various functional groups can be studied for quantification of the degradation [41], here, the focus was on the vinyl groups (—CH=CH_2), which indicate the dominant reaction behavior of the HDPE (chain scission or crosslinking) [18, 24, 25, 41, 42], and the carbonyl groups (—C=O), which quantifies the degree of oxidation occurring to the polymer [43, 44]. The method described by Almond et al. [43] and an adapted method from Mendes et al. [42] were chosen to calculate the carbonyl index (*COI*) and the vinyl index (*VI*), respectively. Almond et al. compared many different methods of calculating *COI* and found that calculating the summed up integral of different oxidation related peaks (from 1650 to 1850 cm^{-1}) is the most reliable way of determining *COI*. The *VI* is calculated by the integration of the spectrum between 875 and 925 cm^{-1} (related to the vinyl absorption peak at 910 cm^{-1}). Both integrals were normalized to the area of the peak of the CH_2-scissoring between 1420 and 1500 cm^{-1}.

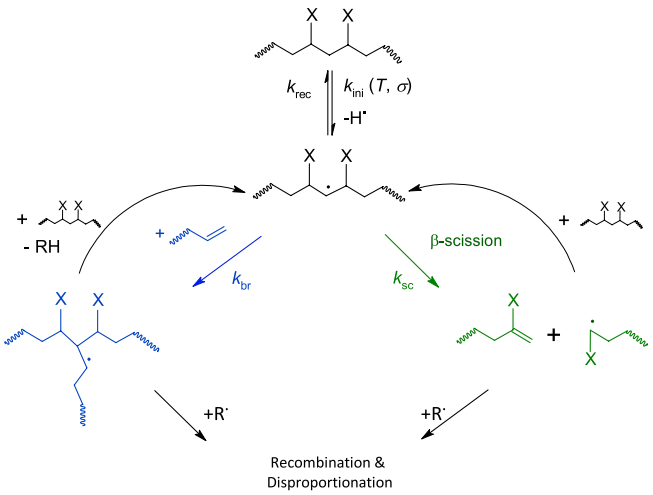

FIGURE 3 | Simplified reaction mechanism of polyolefins and resulting polymeric products applying the assumptions made by Goldberg and Zaikov [7]. [Color figure can be viewed at wileyonlinelibrary.com]

2.5 | Isothermal Oxidation Incubation Time

The isothermal oxidation incubation time (OIT) determines the resistance of the HDPE to oxidation and therefore it can indicate the relative amount of active antioxidants. The OIT was determined using a Netzsch Polyma DSC. For this, 10 mg of a sample were heated to 200°C at 10 K min^{-1} at nitrogen atmosphere (40 mL min^{-1}). After a conditioning of 2 min, an oxygen gas flow (40 mL min^{-1}) was injected to oxidize the HDPE. The OIT was determined according to ISO 11357.

3 | Theory and Calculation

A kinetic model is suggested to quantify the influence of temperature T_{treat}, time t_{treat}, and in-phase shear stress σ'_{treat} on the change in molecular weight due to thermo-mechanical treatment.

Goldberg and Zaikov [7] assumed that degradation of polyolefins is a competition between crosslinking and chain scission. A simplified version of Figure 1 displays this (see Figure 3). The generation of macroradicals from thermo and mechanical

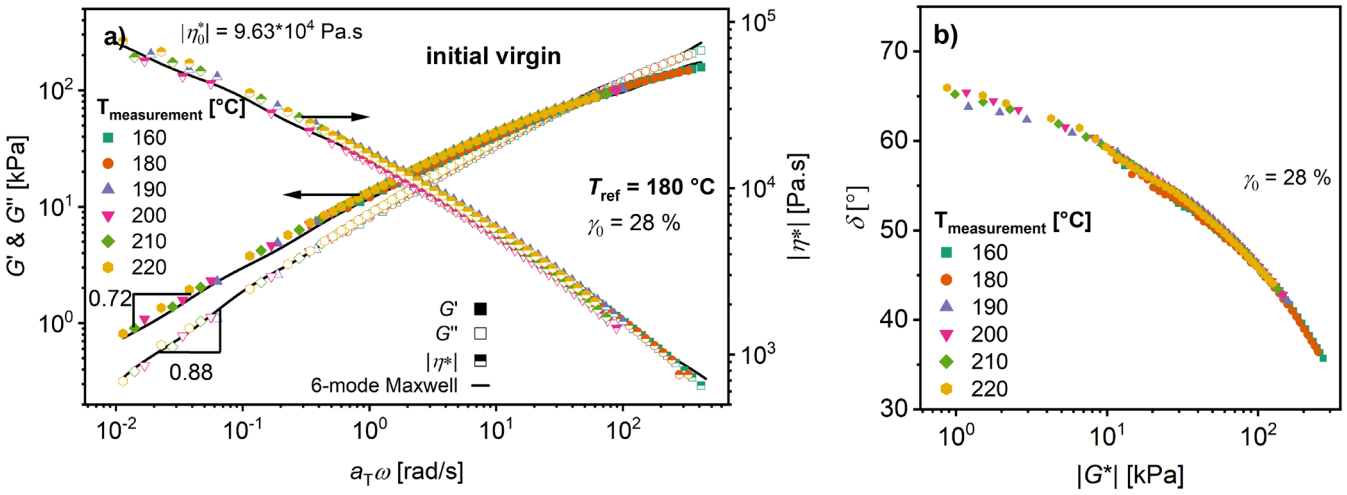

FIGURE 4 | (a) Initial mastercurve (G', G'', and $|\eta^*|$) of virgin HDPE fitted with a 6-mode Maxwell model (solid lines), and gross estimated zero shear viscosity (b) van Gurp–Palmen-plot δ versus $|G^*|$ of the same polymer measured at different temperatures in the linear regime. The frequency sweep at each temperature took 8 min. [Color figure can be viewed at wileyonlinelibrary.com]

TABLE 3 | Maxwell model parameter (6-mode) for studied virgin HDPE at T_{ref} = 180°C.

Modulus g_i (kPa)	Relaxation time λ (s)
336	2.1×10^{-3}
93	2.3×10^{-2}
24	0.21
8.0	1.3
2.2	11
0.51	1.0×10^{2}

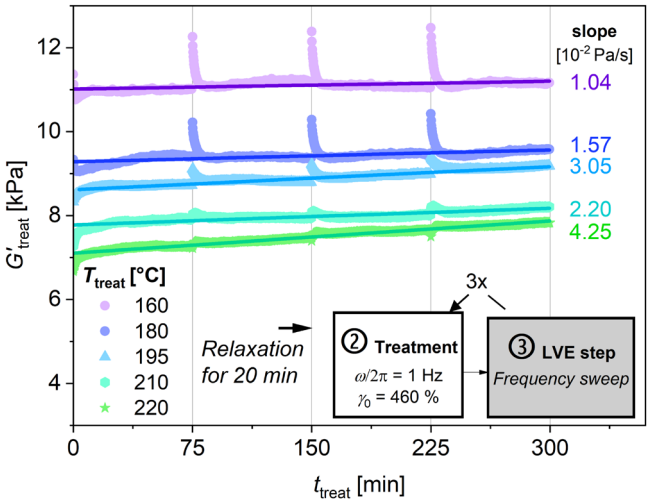

FIGURE 5 | Storage modulus G'_{treat} during the treatment for various temperatures at γ_0 = 460% and $\omega/2\pi$ = 1 Hz. Interruptions were used to measure ω_c in the linear viscoelastic regime. [Color figure can be viewed at wileyonlinelibrary.com]

reaction is merged to one initiation reaction k_{ini} for easier calculation. Furthermore, oxidation is neglected since no significant increase in *COI* (see later) can be seen.

The parameter α is introduced as the relative molecular weight at t_{treat} to the initial molecular weight and is defined as:

$$\alpha\left(t_{treat}, T_{treat}, \sigma'_{treat}\right) = \frac{M_0}{M\left(t_{treat}, T_{treat}, \sigma'_{treat}\right)} \tag{3}$$

where M_0 and $M(t_{treat})$ are the number-average molecular weight of the virgin HDPE, and after t_{treat}, respectively. A value of $\alpha < 1$ represents an increase in the molecular weight, and vice versa.

Goldberg and Zaikov used the following equation to calculate the change in the molecular weight:

$$\frac{d\alpha}{dt_{treat}} = \frac{d\frac{M_0}{M(t_{treat})}}{dt_{treat}} = \sqrt{\frac{k_{ini}}{k_{rec}}} * \frac{k_{sc} - \left(k_{br} * c_{C=C}\right)}{c_{M,0}} \tag{4}$$

where k_{rec} is the rate of recombination of two radicals, k_{sc} is the rate of β-scission, and k_{br} is the rate of branching. The temperature dependence of each rate is described by a simple Arrhenius equation. The $c_{C=C}$ denotes the concentration of double bonds in the polymer in mol L^{-1} and k_{ini} stands for the rate of the initiation reaction, which describes the formation of radicals, caused by T_{treat} and σ'_{treat}. The c_M describes the initial concentration of the polymer in mol L^{-1}, which results from the normalization by M_0. It is calculated by the density of the polymer melt, which is assumed as 0.76 g cm^{-3} at T = 180°C [45].

To describe the merged effect of T_{treat} and σ'_{treat} on the rate of the initiation reaction k_{ini}, Equation (5) as derived from

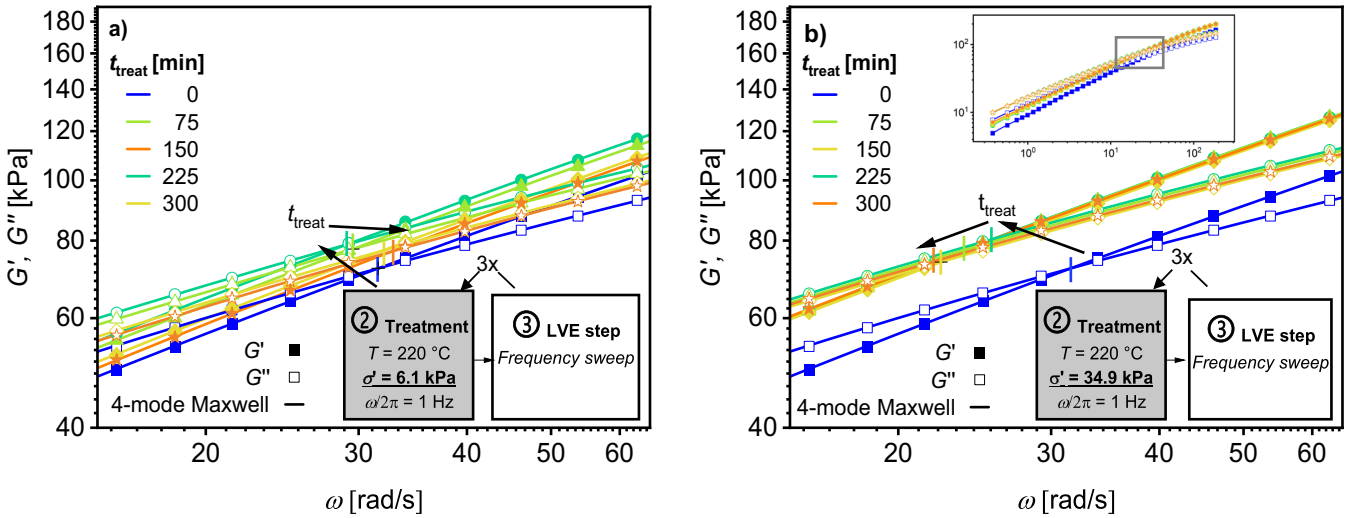

FIGURE 6 | G', G'', and resulting ω_c measured in LVE-regime during and after a treatment at (a) low σ'_{treat} = 6.1 kPa at 220°C and (b) high σ'_{treat} = 34.9 kPa at T_{treat} = 220°C. Solid lines are fitted curves with four-mode Maxwell-model for G' and G″. The crossover point is determined using the respective Maxwell fits. Results of ω_c with respect to t_{treat} are shown for both in Figure 7a. [Color figure can be viewed at wileyonlinelibrary.com]

Zhurkov [8] is used. The equation describes the reduction of the activation energy $E_{a,ini}$ for the formation of macroradicals, caused by the applied stress. This semi-empirical relation lowers $E_{a,ini}$ of a chemical reaction via the in-phase shear stress.

$$k_{ini} = k_{0,ini} * \exp\left(- \frac{E_{a,ini} - \beta \times \sigma'_{treat}}{R \times T_{treat}} \right) \quad (5)$$

where $k_{0,ini}$ is a pre-exponential coefficient, $E_{a,ini}$ is the activation energy of the initiation reaction, R is the universal gas constant, T_{treat} is the absolute temperature in Kelvin, β is the volume factor in $J\,Pa^{-1}\,mol^{-1}$. The amplitude of the applied in-phase shear stress during treatment is denoted with σ'_{treat} in $N\,m^{-2}$. The unit of β results with $m^3\,mol^{-1}$ and therefore β represents formally an inverse number concentration.

4 | Results and Discussion

4.1 | Rheological Measurements on Virgin HDPE

In this article, the thermo-mechanical treatment is studied for a specific HDPE sample using a closed-cavity rheometer (CCR). As described earlier, changes in rheological data are measured by the described treatment in LVE regime. There are various values, which can be used to monitor a change in the average molecular weight via the following parameters: zero shear viscosity $|\eta_0^*|$, the pivot point of the complex viscosity versus angular frequency, and the crossover angular frequency ω_c [46, 47]. Linear polyethylene shows a low flow activation energy ($E_{a,flow} = 22$–$30\,kJ\,mol^{-1}$), which increases up to $80\,kJ\,mol^{-1}$ with the amount of branching [48] (here, $E_{a,flow} \approx 35\,kJ\,mol^{-1}$). Additionally, it shows a rather narrow temperature window for

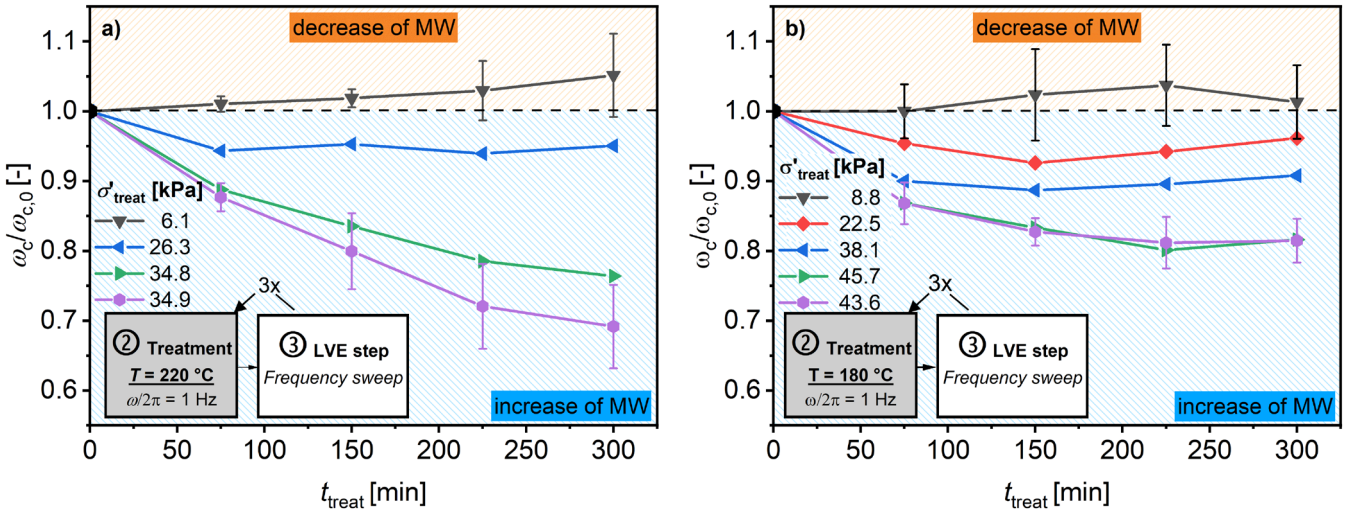

FIGURE 7 | Normalized ω_c (compared with the virgin HDPE, $\omega_c/\omega_{c,0}$) measured in LVE at various applied σ'_{treat} as a function of the summed up t_{treat} at (a) $T_{treat} = 220°C$ and (b) $T_{treat} = 180°C$. Standard deviation is given for the parameter sets, which were repeated three times each with a new sample. Results for further T_{treat} are shown in Figure S1. [Color figure can be viewed at wileyonlinelibrary.com]

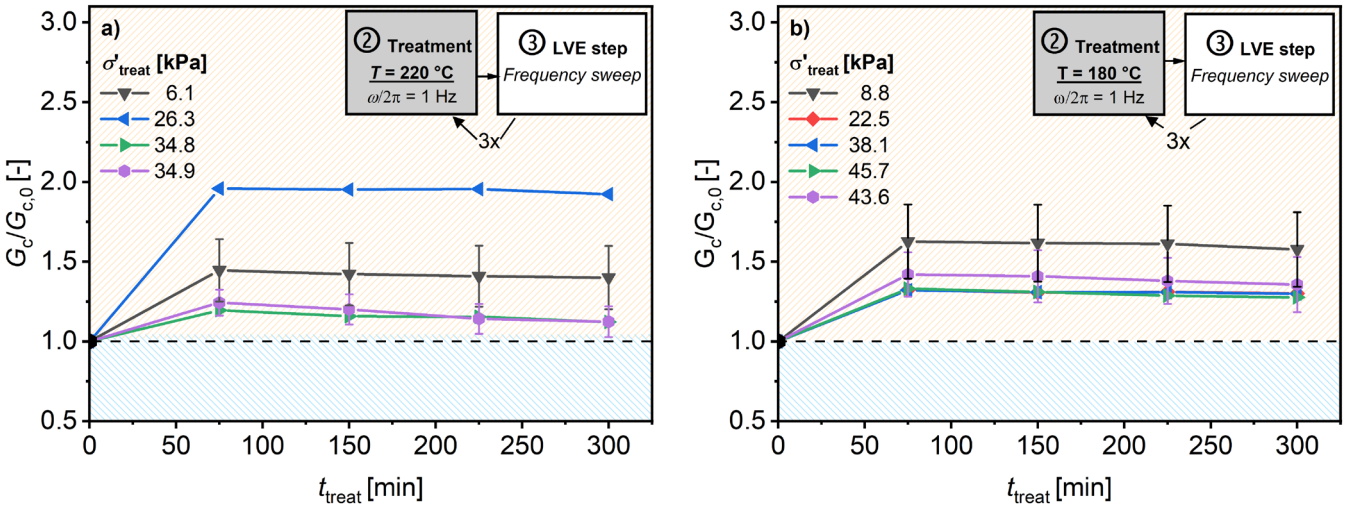

FIGURE 8 | Normalized G_c (compared with the virgin HDPE, $G_c/G_{c,0}$) measured in LVE at various applied σ'_{treat} as a function of the summed up t_{treat} at (a) $T_{treat} = 220°C$ and (b) $T_{treat} = 180°C$. Standard deviation is given for the parameter sets, which were repeated three times each with a new sample. Results for further T_{treat} are shown in Figure S2. [Color figure can be viewed at wileyonlinelibrary.com]

the measurement since crystallization and degradation limit the usable temperature regime ($T_{melting} < T_{measurement} < T_{degradation}$) [49]. Because of these two reasons, a calculated mastercurve using time temperature superposition (TTS) does not broadly expand the range of angular frequency, which can be measured in a fixed time.

The mastercurve (calculated using TTS) of G' and G'' of the virgin HDPE is shown in Figure 4a. The Maxwell parameters for this material are shown in Table 3. The so called van Gurp–Palmen-plot (loss angle δ as a function of the absolute value of complex modulus $|G^*|$) [50, 51] in Figure 4b clarifies that TTS is applicable because the curve appears continuous and its derivative is continuous. As Figure 4a shows, the plateau for the absolute value of the complex viscosity$|\eta^*|$ at low $\omega = 0.01\,\mathrm{rad\,s^{-1}}$ is not reached. The slopes of d(log(G')) over d(log(ω)) = 0.88 and d(log(G'')) over d(log(ω)) = 0.72 confirm this. Consequently, the determination of $|\eta_0^*|$ and the pivot point would be inaccurate. Hence, the change in the ω_c and the G_c will be investigated to analyze potential changes in the molecular weight and the molecular weight distribution, respectively (Table 3).

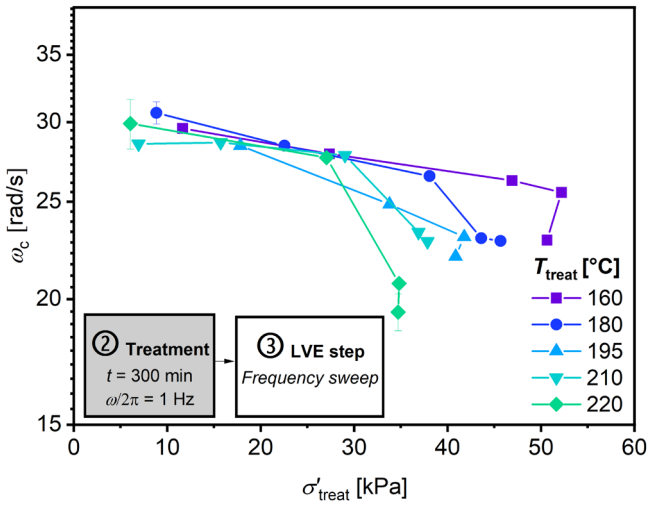

FIGURE 9 | Determined cross over angular frequency ω_c after the treatment step at given σ'_{treat} and T_{treat} after $t_{treat} = 300\,\mathrm{min}$. The decrease in ω_c is pronounced at higher σ'_{treat} and T_{treat}. This decrease in ω_c indicates an increase in M_w. The extruded HDPE shows a ω_c of $25.4\,\mathrm{rad\,s^{-1}}$. [Color figure can be viewed at wileyonlinelibrary.com]

4.2 | Rheological Investigations During and After the Thermo-Mechanical Treatment

During the thermo-mechanical treatment (see Figure 2), $G'_{treat}(\omega/2\pi = 1\,\mathrm{Hz})$ can be measured online as a function of time, t_{treat} for defined temperature $T_{treat} = (160°C–220°C)$ and applied shear strain $\gamma_{0,treat} = (28\%–460\%)$. As can be seen in Figure 5, G'_{treat} increases with time for all temperatures. The slope of G'_{treat} with respect to t_{treat} increases from $1.04 \times 10^{-2}\,\mathrm{Pa\,s^{-1}}$ for $T_{treat} = 160°C$ to $4.25 \times 10^{-2}\,\mathrm{Pa\,s^{-1}}$ for $T_{treat} = 220°C$ at the given frequency and amplitude, which is approximately a factor of four. However, these data are not adequate for quantitative analysis, because all measurements shown in Figure 5 are conducted in the nonlinear viscoelastic regime. Additionally, higher T_{treat} results in the applied frequency shifting toward to the terminal regime and the measurements at higher T_{treat} might be more sensitive to changes in the molecular weight.

Additionally, ω_c and G_c were determined with a frequency sweep in the LVE between and after the treatments, for temperatures from $T_{treat} = 160°C–220°C$. Figure 6 shows the results of treatments at $T_{treat} = 220°C$ under (a) a low $\sigma'_{treat} = 6.1\,\mathrm{kPa}$ and (b) a high $\sigma'_{treat} = 34.9\,\mathrm{kPa}$, which correspond to the highest and lowest amplitudes, respectively. Note that the average σ'_{treat} is used to quantify this parameter.

The results for normalized ω_c relative to $\omega_{c,0}$ ($\omega_c/\omega_{c,0}$) as a function of t_{treat} are shown in Figure 7 for (a) $T_{treat} = 220°C$ and (b) $T_{treat} = 180°C$. Figure 8 shows the normalized G_c relative to $G_{c,0}$

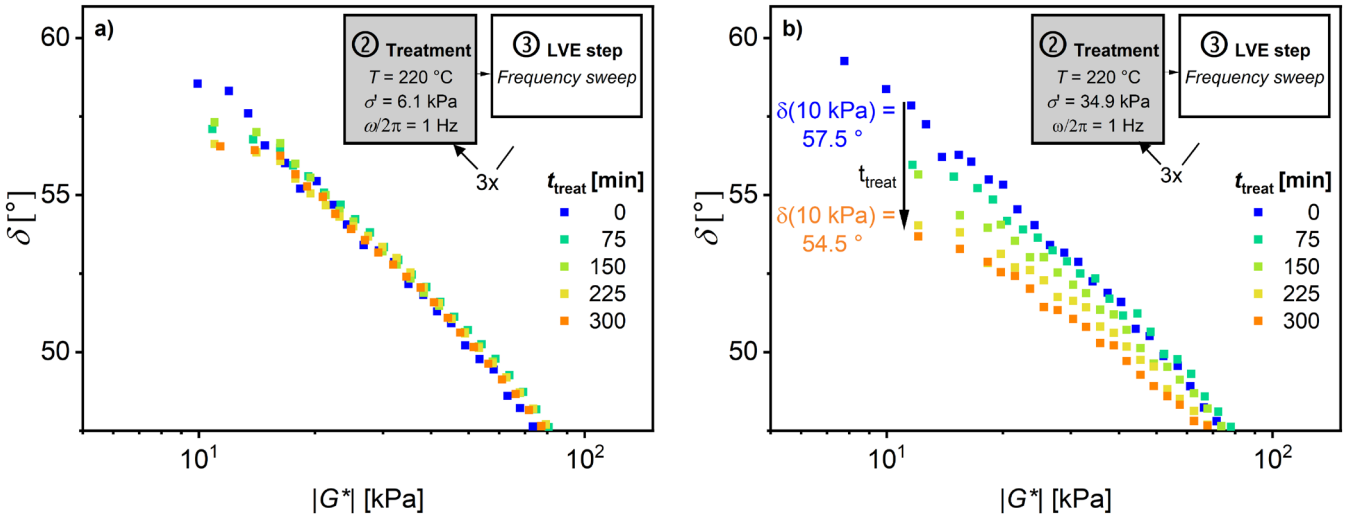

FIGURE 10 | Van Gurp–Palmen-plot measured in LVE regime after a treatment at (a) low $\sigma'_{treat} = 6.1\,\mathrm{kPa}$ and (b) high $\sigma'_{treat} = 34.9\,\mathrm{kPa}$, both at $T_{treat} = 220°C$ for indicated t_{treat}. (a) No clear difference between virgin and thermo-mechanical treated HDPE, while (b) shows a clear decrease in the loss angle δ at low $|G^*|$. This indicates an influence of the shear stress on the change of rheological properties, specifically to a higher elasticity. [Color figure can be viewed at wileyonlinelibrary.com]

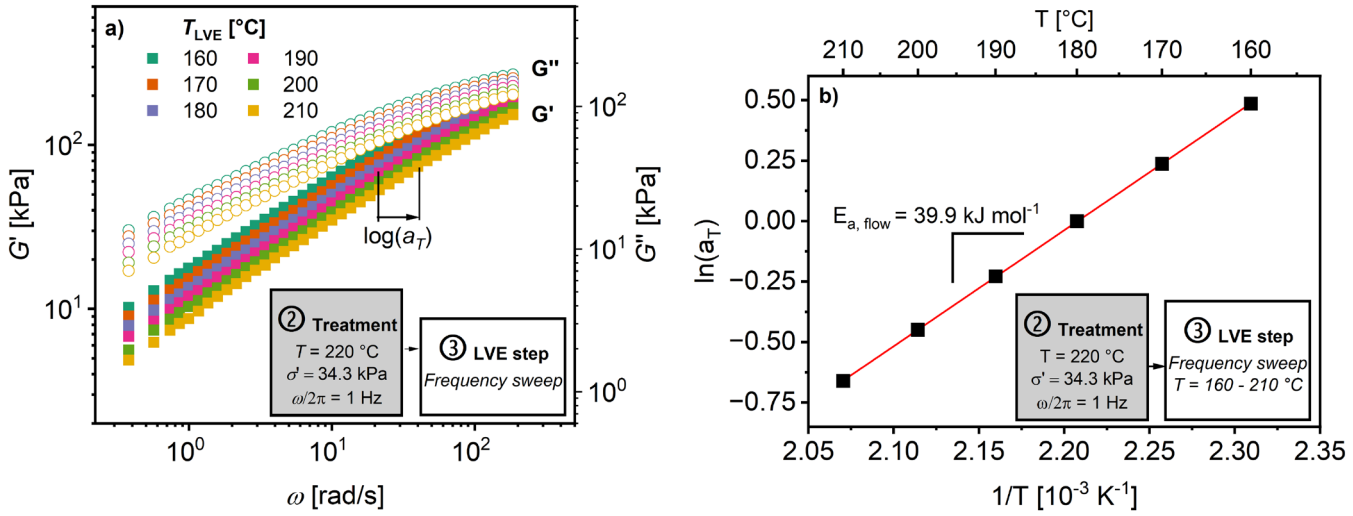

FIGURE 11 | (a) Results of frequency sweep and example of the determination of $\log(a_T)$ and (b) $\ln(a_T)$-values determined ($\ln(a_T) = 2.303 \log(a_T)$) with respect to inverse temperature and calculation of the flow activation energy ($E_{a,flow}$) by determining the slope $\ln(a_T)$ and multiplying it by $R = 8.314\,J\,mol^{-1}\,K^{-1}$. [Color figure can be viewed at wileyonlinelibrary.com]

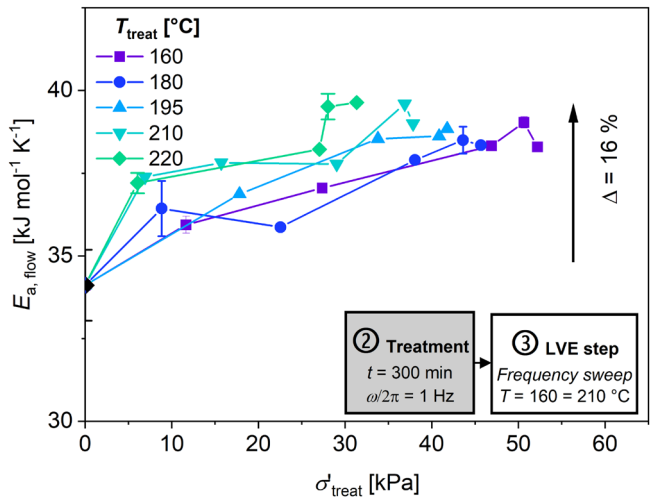

FIGURE 12 | Determined activation energies resulting from $\ln(a_T)$ by TTS for calculating the mastercurve using the Arrhenius equation; activation energies are shown with respect to their applied σ'_{treat} during $t_{treat} = 300\,min$ and given T_{treat}. The virgin HDPE is shown at $\sigma' = 0\,kPa$. The extruded HDPE shows an $E_{a,flow}$ of $38.5\,rad\,s^{-1}$. [Color figure can be viewed at wileyonlinelibrary.com]

($G_c/G_{c,0}$) under the same conditions. Selected procedures were repeated three times with new samples to quantify reproducibility. These results are shown with their respective standard deviations. The results for the other studied temperatures can be found in the Supporting Information. The result after the extrusion of the HDPE is provided in the caption of this figure. This is because no uniform σ'_{treat} can be calculated for extrusion.

The evolution of $\omega_c/\omega_{c,0}$ strongly depends on the σ'_{treat}. The higher the σ'_{treat} the greater the decrease in resulting $\omega_c/\omega_{c,0}$. Additionally, the higher the T_{treat} also the higher the decrease in $\omega_c/\omega_{c,0}$. This decrease in $\omega_c/\omega_{c,0}$ indicates a detectable increase in the measured molecular weight. Therefore, the resulting molecular weight should be a function of T_{treat}, t_{treat}, and σ'_{treat}.

Figure 9 summarizes the resulting ω_c with respect to the applied σ'_{treat} after $t_{treat} = 300\,min$. It can be observed that ω_c decreases with higher σ'_{treat} for temperatures from 160°C to 220°C, as expected from Equations (4) and (5).

This observation can be explained by an increased rate of the dominant reaction (here chain branching) due to a higher rate of the initiation reaction, which is influenced by σ'_{treat} according to Equation (4). The related reaction kinetics are discussed and quantified below.

Trinkle and Friedrich used the van Gurp–Palmen-plot (δ vs. $|G^*|$) to analyze the polydispersity $Đ$ and long-chain branching (LCB) molecular architecture of polyolefin (HDPE, PP) melts [50, 51]. Figure 10 shows the van Gurp–Palmen-plot for the same samples as those in Figure 6 (results at further T_{treat} be found in Figure S3). The sample that was exposed to $\sigma'_{treat} = 34.9\,kPa$ and $T_{treat} = 220°C$ (b) shows a decrease in the loss angle δ of 3° at low $|G^*| = 10\,kPa$. The loss angle of the sample exposed to low $\sigma'_{treat} = 6.1\,kPa$ (a) displays no detectable change.

A decrease in the loss angle δ can result from an increase in $Đ$ as well as from an increase in long-chain branching (LCB) of the polymer [50, 51]. The HT-SEC results (see below) do not show an increase in $Đ$ of all samples. Hence, the decrease in the loss angle δ in the van Gurp–Palmen-plot indicates an increase in the LCB content. Measurements using HT-SEC coupled to a multiangle light scattering (MALS-) detector would be necessary to address this hypothesis [52].

The activation energy of flow, $E_{a,flow}$, is used to assess the change in molecular structure after each treatment and to confirm this hypothesis. Therefore, the shift factor $\log(a_T)$, which results from calculating the mastercurve in the LVE regime, is used [53]. This is shown in Figure 11a. The shift factor $\log(a_T)$ is related to the inverse temperature by applying a simple Arrhenius equation [54]. The flow activation energy is defined as the slope of $\ln(a_T)$ with respect to T^{-1} (in K^{-1}) multiplied by the universal

gas constant ($R = 8.314\,\mathrm{J\,mol^{-1}\,K^{-1}}$) (Figure 11b). Figure 12 shows the flow activation energy $E_{a,flow}$ for the samples after the thermo-mechanical treatment. The result after the extrusion of the HDPE is provided in the caption of this figure.

An increase in $E_{a,flow}$ of up to 16% can be observed after a treatment at higher σ'_{treat} for all T_{treat}. According to the literature, an increase in the activation energy indicates a higher degree of branching [54–57]. To compare this results shows Table 4 the $E_{a,flow}$ from the literature, where changes in $E_{a,flow}$ due to LCB are studied for various HDPEs.

The measured increase in $E_{a,flow}$ and the decrease in the concentration of vinyl groups (see below) suggest that the treatment at a high stress leads to an increase in branching. Additionally, the results from the van Gurp–Palmen-plots and from elongation viscosity, which are shown later, suggest that the branching is long-chain branched (LCB).

4.3 | Elongation Viscosity After Thermo-Mechanical Treatment

The uniaxial elongation rheology measurements are shown in Figure 13 for both (a) the virgin HDPE and (b) the sample treated at $T_{treat} = 220°C$, $\sigma' = 34.8\,kPa$, and $t_{treat} = 300\,min$. The strain hardening factor (SHF) was determined using the following equation according to Auhl et al. [33].

$$SHF\left(\dot{\varepsilon} = 1\,s^{-1}, \varepsilon = 2.7\right) = \frac{\eta_e^+(t,\dot{\varepsilon})}{\eta_{LVE}^+(t,\dot{\varepsilon})} \tag{6}$$

where ε is the Hencky strain, $\dot{\varepsilon}$ is the Hencky rate, η_e^+ is the elongation viscosity and η_{LVE}^+ is the viscosity determined in the LVE regime. The results for the samples treated under the same conditions as those shown later for SEC are summarized in Table 5.

TABLE 4 | Brief literature review.

Authors	$E_{a,flow}$ (HDPE, linear) and $E_{a,flow}$ (HDPE, LCB) ($kJ\,mol^{-1}$)	Change in $E_{a,flow}$ (LCB) (%)	Change in LCB via ^{13}C-NMR (ΔLCB [1000 C^{-1}])	Sample	Lit. reference
Bersted	23.0 28.6	+14.5	0.02	HDPE with 0.02% of peroxide	[55]
Wood-Adams et al.	27.5 30.7	+11.6	0.011	Diff. HDPE	[54]
	27.5 35.5	+29.1	0.016		
Stadler et al.	27.5 38.0	+38.2	Very low[a]	Diff. HDPE	[57]

Note: Change in flow activation energy of HDPEs with a defined concentration of LCB (determined by ^{13}C-NMR) compared to the respective linear HDPE.
[a]No numerical data are given in this article.

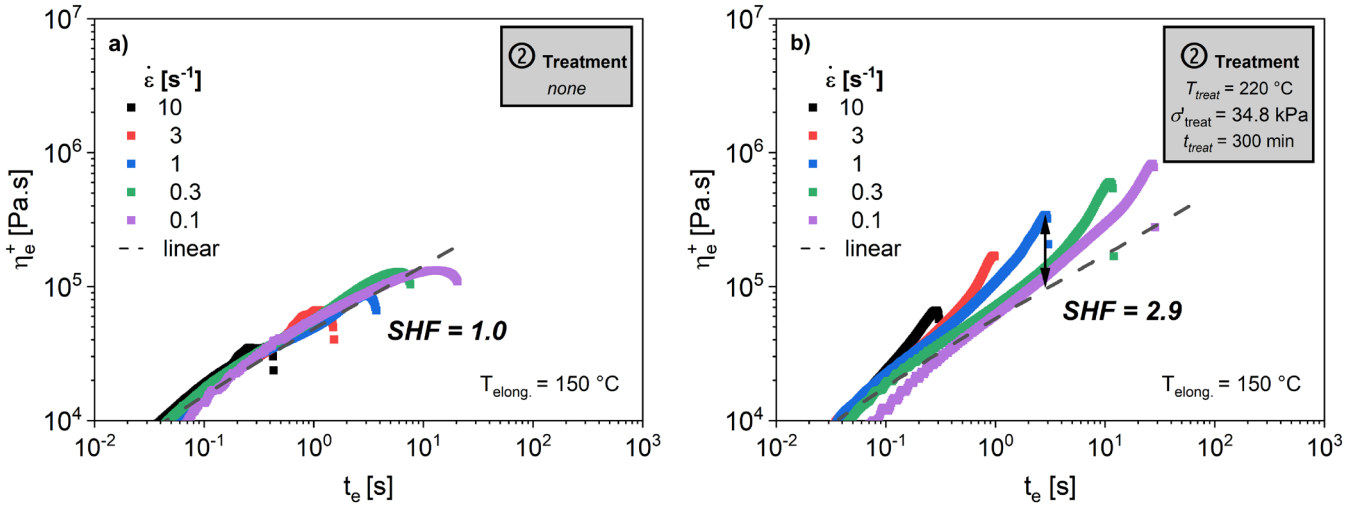

FIGURE 13 | Elongation viscosity over elongation time for (a) virgin HDPE and (b) at given conditions treated HDPE and their respective shear rheology data from measured in LVE-regime both at 150°C. The SHF was determined at an Hencky strain $\varepsilon = 2.7$ and Hencky rate $\dot{\varepsilon} = 1\,s^{-1}$ according to Equation (7). [Color figure can be viewed at wileyonlinelibrary.com]

The results indicate that there is no significant strain hardening in the virgin HDPE. However, the samples subjected to the thermo-mechanical treatment in the closed-cavity rheometer show a SHF = 2.9. The extruded sample shows a SHF = 3.3. According to Ahirwal et al., these results confirm that thermo-mechanical treatment leads to an increase of long chain branching of this HDPE [58].

4.4 | Molecular Characterization After Thermo-Mechanical Treatment

While a change in the rheological properties can be observed in situ after each treatment step, it is crucial to verify that these changes are based on changes in molecular weight or molecular topology rather than systematic effects arising from the polymer flow in the utilized rheometer or reversible effects after mechanical treatment, as reported in previous studies for branched polyethylene [59, 60]. High-temperature size exclusion chromatography (HT-SEC) and FTIR are established methods [3, 15, 16, 18, 25] for investigating polymer degradation on a molecular level. Another spectroscopic method to quantify branching is ^{13}C-NMR [54, 61], which is not covered in this article.

TABLE 5 | Stain hardening factors (SHF) of the virgin material and after the thermo-mechanical treatment at the respective conditions.

ID	T_{treat} (°C)	σ'_{treat} (kPa)	t_{treat} (min)	SHF (-)
1	—	—	—	1.0
2	180	43.6	300	1.3
3	195	40.9	300	1.8
4	220	6.1	300	1.4
6	220	34.8	300	2.9
EX	190[b]	94.9[a]	35	3.3

Note: The SHF was determined at an Hencky strain $\varepsilon = 2.7$ and Hencky rate $\dot{\varepsilon} = 1\,s^{-1}$ according to Equation (7). There is no value for the sample with ID 5.
[a]Temperature of melt during extrusion with parameters given in Chapter 2.1.
[b]Shear stress calculated using Equation (2), as the total shear stress.

4.4.1 | HT-SEC and Correlation With Rheological Results

HT-SEC analysis was carried out for the virgin HDPE (ID 1), the extruded sample (ID EX) and for five different treated samples of the investigated HDPEs (ID 2 to 6). The results are shown in Table 6 and Figure 14. Table 6 demonstrates that all samples show a clear increase in M_n and M_w compared with the virgin HDPE. The samples with ID 4 and ID 6 show the highest increase in molecular weight. This increase of 12.8% for M_n and of 11.2% for M_w for the sample with ID 6 agrees with the literature data shown (Table 4), where increases of M_w of around 17% are reported after multiple extrusion. These results confirm the rheological results that the thermo-mechanical treatment leads to an increase in molecular weight at certain conditions.

The values M_n and M_w (determined with HT-SEC) are correlated with the measured ω_c in Figure 15a,b, respectively. There is a correlation of $R^2 = 0.86$ for ω_c with respect to M_n and $R^2 = 0.84$ for ω_c with respect to M_w (excluding sample ID 4) with the simplest scaling law determined for a reptating, linear polymer chain, which is an exponent of −3.4 as reported in the literature [47]. However, the sample ID 4 shows a larger deviation from this simple scaling law. Note, that this scaling law is expected for a linear monodisperse homopolymer [47]. Therefore, it would be useful to investigate the sample ID 4 using a HT-SEC connected to a MALS-detector to determine whether the deviation of the HT-SEC data from rheology is due to different branching structure of the sample [52].

Figure 15b shows the measured crossover modulus G_c against $Đ$ determined by HT-SEC. No clear correlation between the data is observed. This might origin in the broad distribution of the investigated HDPE that showed only a minor change.

TABLE 6 | Studied samples and their respective parameters of thermo-mechanical treatment.

ID	T_{treat} (°C)	σ'_{treat} (kPa)	t_{treat} (min)	M_n (kg mol^{-1})	Reproducibility (kg mol^{-1})	M_w (kg mol^{-1})	Reproducibility (kg mol^{-1})	$Đ$ (-)
1	—	—	—	11.7	±0.3	108.1	±2.6	9.2
2	180	43.6	300	12.7	—[a]	117.5	—[a]	9.2
3	195	40.9	300	13.1	—[a]	120.0	—[a]	9.2
4	220	6.1	300	13.8	±1.7	119.5	±5.7	8.7
5	220	34.8	75	12.6	±0.2	116.5	±0.2	9.1
6	220	34.8	300	13.2	±0.2	120.6	±0.9	8.9
EX	190[b]	94.9[c]	35	12.7	±0.3	117.3	±2.6	9.2

Note: Resulting number-average molecular weight M_n, weight-average molecular weight M_w, and dispersity $Đ$ of virgin and treated HDPE. The results are the average from two HT-SEC measurements: The reproducibility is calculated as the difference between average and maximum value.
[a]Samples were measured only once.
[b]Temperature of melt during extrusion with parameters given in Chapter 2.1.
[c]Shear stress calculated using Equation (2), as the total shear stress.

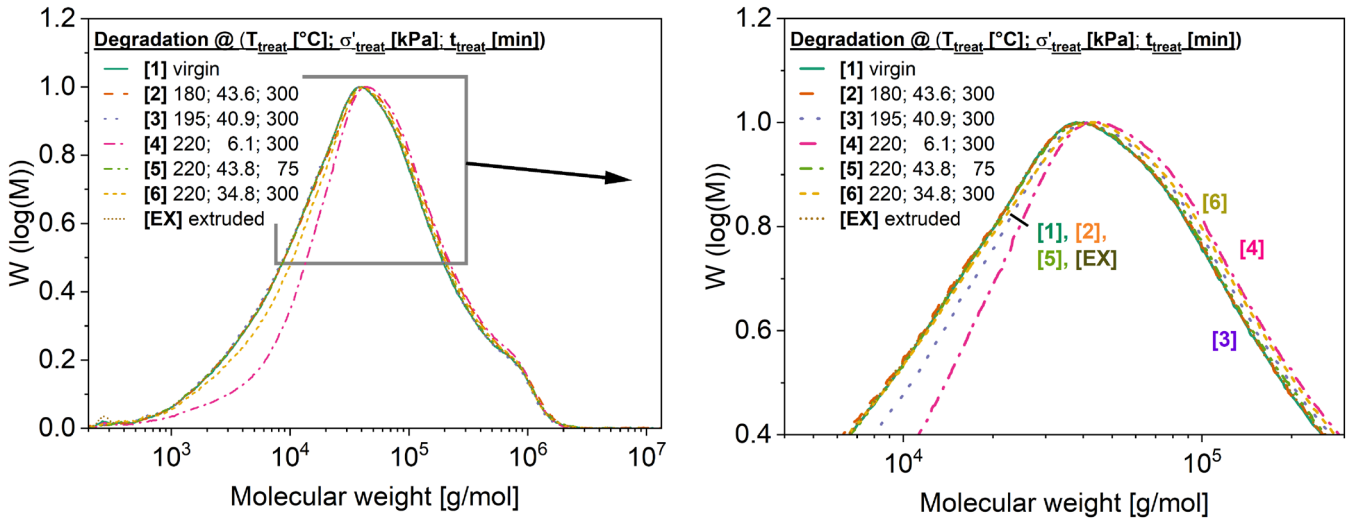

FIGURE 14 | Molecular weight distribution of ID 1, the virgin HDPE; ID 3–ID 6, HDPE subjected to various thermo-mechanical treatment; and ID EX, the extruded sample, see Table 5. The molecular weight distribution was determined via HT-SEC. Results are normalized to the integral of the curve. An IR-detector at 2920 cm^{-1} was used. [Color figure can be viewed at wileyonlinelibrary.com]

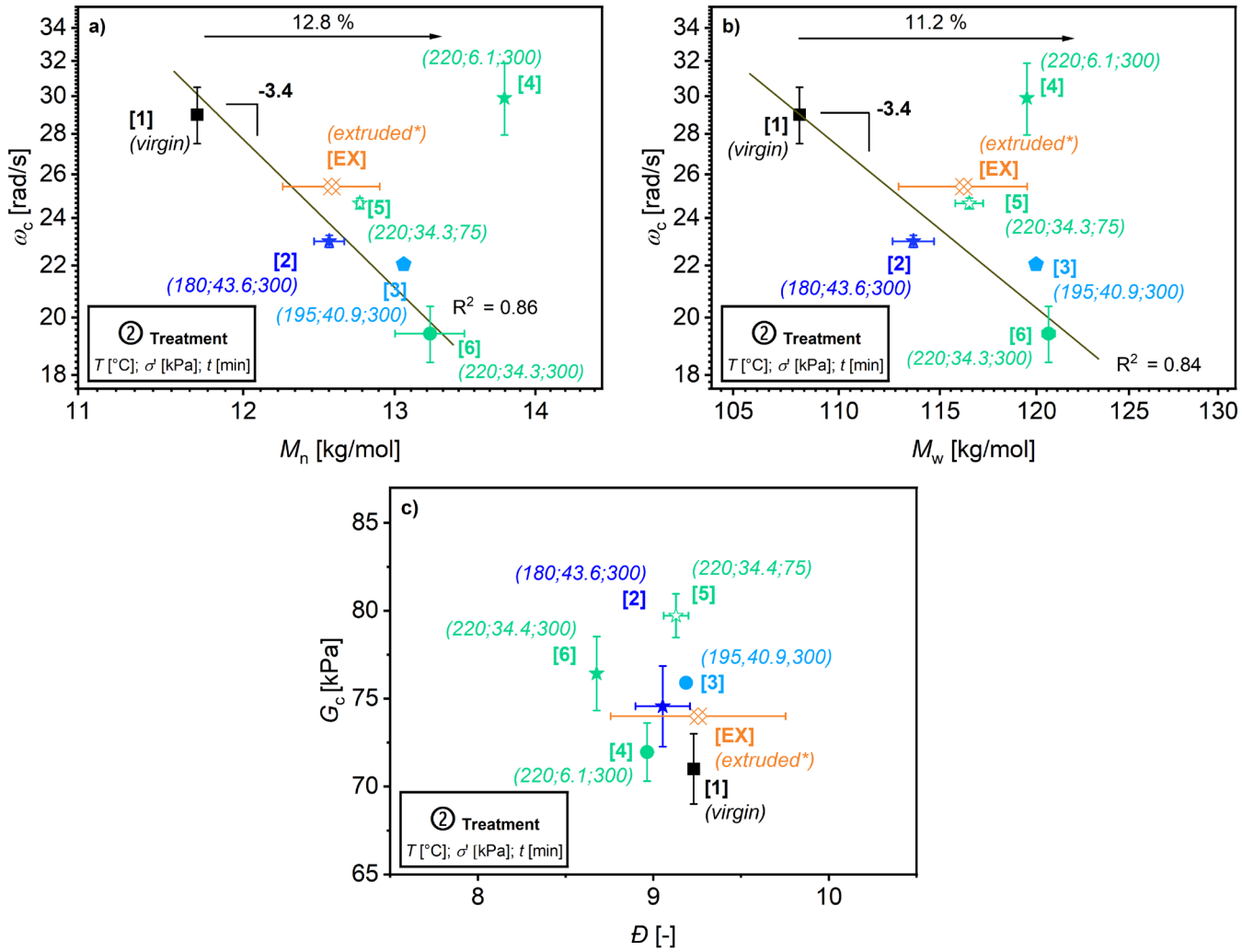

FIGURE 15 | (a) Relation between rheologically measured ω_c and M_n measured with HT-SEC, with the scaling law −3.4, (b) same with M_w and (c) rheologically measured G_c with respect to $Đ$ measured with HT-SEC. All samples were treated under the shown conditions during the treatment step. [Color figure can be viewed at wileyonlinelibrary.com]

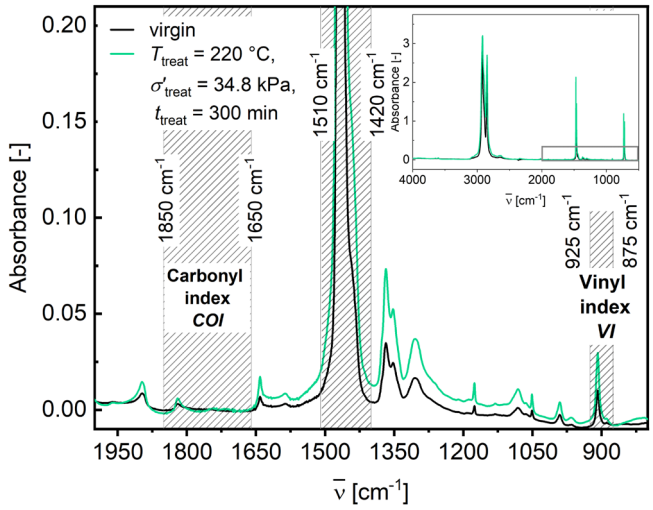

FIGURE 16 | FTIR-spectra before (black) and after treatment step at T_{treat} = 220°C and σ'_{treat} = 34.8 kPa (green). The drawn lines represent the boundaries for the peak integration for *COI* (1850–1650 cm^{-1}) and the boundaries for the peak integration for *VI* (875–925 cm^{-1}), respectively. Both integrals were normalized to the integral of the spectrum between 1510 and 1420 cm^{-1}, which is related to the CH_2-scissoring. The measurement was conducted using transmission at room temperature. [Color figure can be viewed at wileyonlinelibrary.com]

4.4.2 | FTIR Spectroscopy

The use of FTIR gives insights into degradation mechanisms like chain scission, chain branching, and oxidation [18, 24, 25, 41–44]. The IR spectra of the virgin HDPE and after a treatment at T_{treat} = 220°C, σ'_{treat} = 34.8 kPa, and t_{treat} = 300 min are given in Figure 16.

Figure 16 illustrates the spectral boundaries for the calculation of the vinyl index (*VI*) and the carbonyl index (*COI*) via spectral integration. The results are plotted against σ'_{treat} in Figure 17 (a) for VI and (b) for COI.

To analyze the dominant reaction VI is used. A decreasing *VI* indicates an increase in branching of the polymer, because the vinyl group reacts with radicals resulting in a branching point [25].

Figure 17 (a) displays a *VI* = 0.013 of the virgin HDPE. This indicates that the virgin HDPE already shows a certain concentration of vinyl groups of the polymer of 0.042 mol L^{-1} (applying the Lambert–Beer law and the related extinction coefficient (ε = 12 m^2 mol^{-1}) [40]). These initial vinyl groups are likely to result from the polymerization conditions of the HDPE. The *VI* decreases at higher σ'_{treat} > 25 kPa at T_{treat} = 210°C and 220°C by

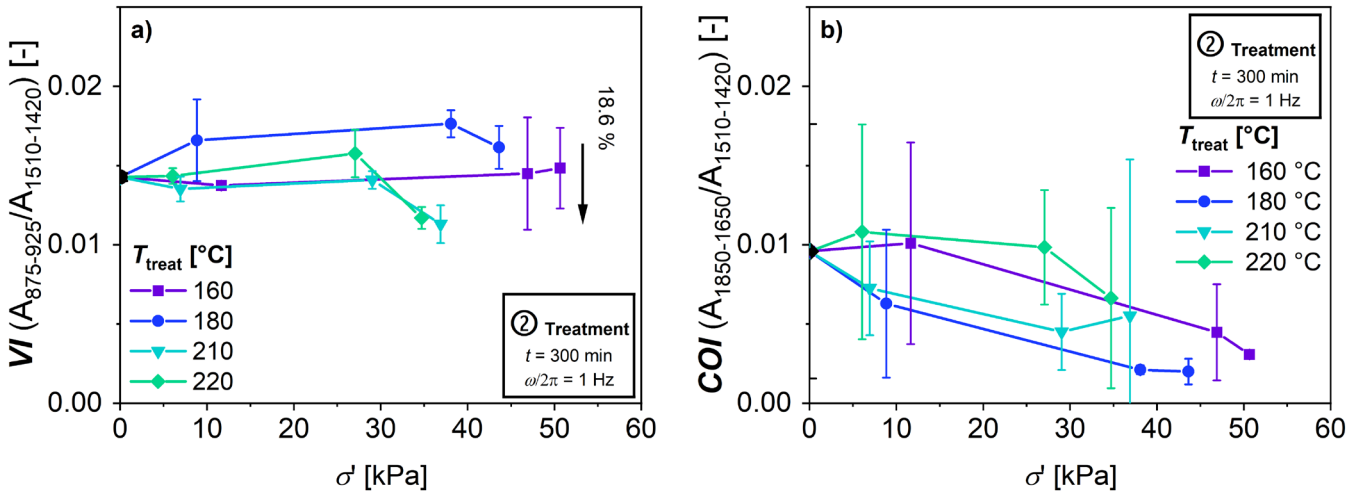

FIGURE 17 | Correlation of (a) *VI* and (b) *COI* to the applied σ' during the treatment step at given temperatures. The virgin HDPE is additionally shown at σ' = 0 kPa. *VI* and *COI* indicate the concentration of vinyl groups and the concentration of the oxidation-related groups, respectively. [Color figure can be viewed at wileyonlinelibrary.com]

TABLE 7 | Comparison of change in molecular weight, *VI*, and *COI* for HDPE in the literature and this article. The conditions from the literature references are shown in Table 1.

Authors	Change in M_w (%)	Change in *VI*[a] (%)	Change in *COI*[a] (%)	Lit. reference
Pinheiro et al.	+17	−26	+400	[25]
Pinheiro et al.	+21	−30	+100	[6]
Moss et al.	+17	−14	—	[16]
This article (T_{treat} = 220°C, σ'_{treat} = 34.4 kPa, t_{treat} = 300 min)	+11.2	−18.6	0	

[a]*VI* and *COI* are different determined compared with this article, but the same peaks were investigated.

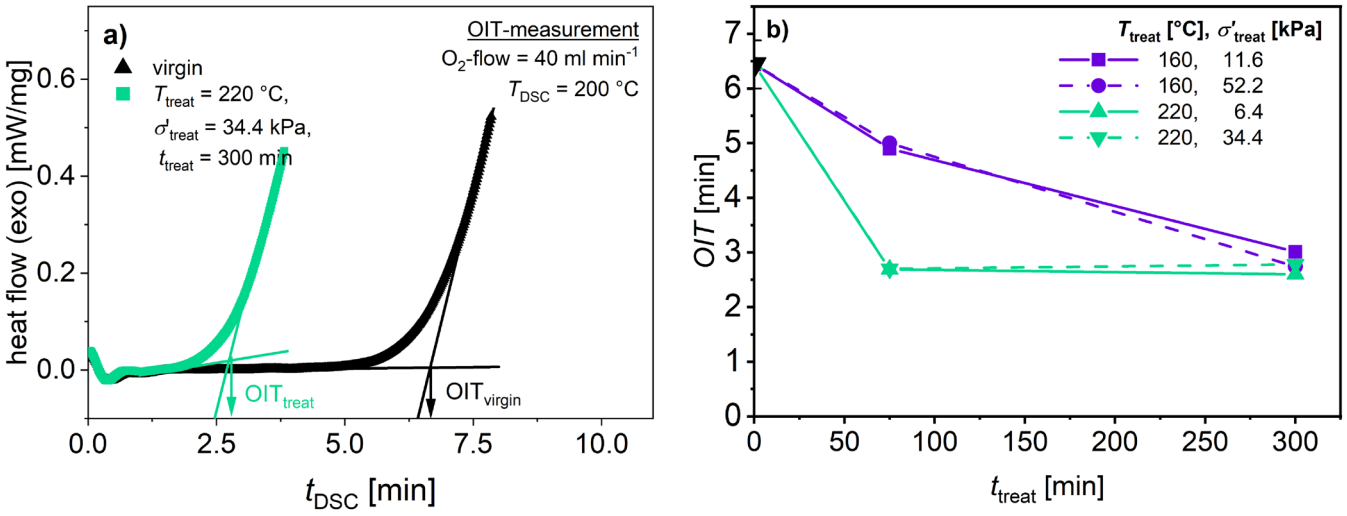

FIGURE 18 | (a) Heat flow at OIT-measurement of the virgin HDPE (black) and a thermo-mechanical treated HDPE (green). The OIT is determined as the crossover of the baseline and the tangent of the exothermic heat flow during oxidation. (b) The results of OIT for different treated samples, at the given low (solid lines) and high (broken lines) σ'_{treat} at T_{treat} = 160°C (purple) and 220°C (green). The OIT indicates the concentration of the reactive antioxidants in the polymer. The virgin HDPE is shown at σ' = 0 kPa. [Color figure can be viewed at wileyonlinelibrary.com]

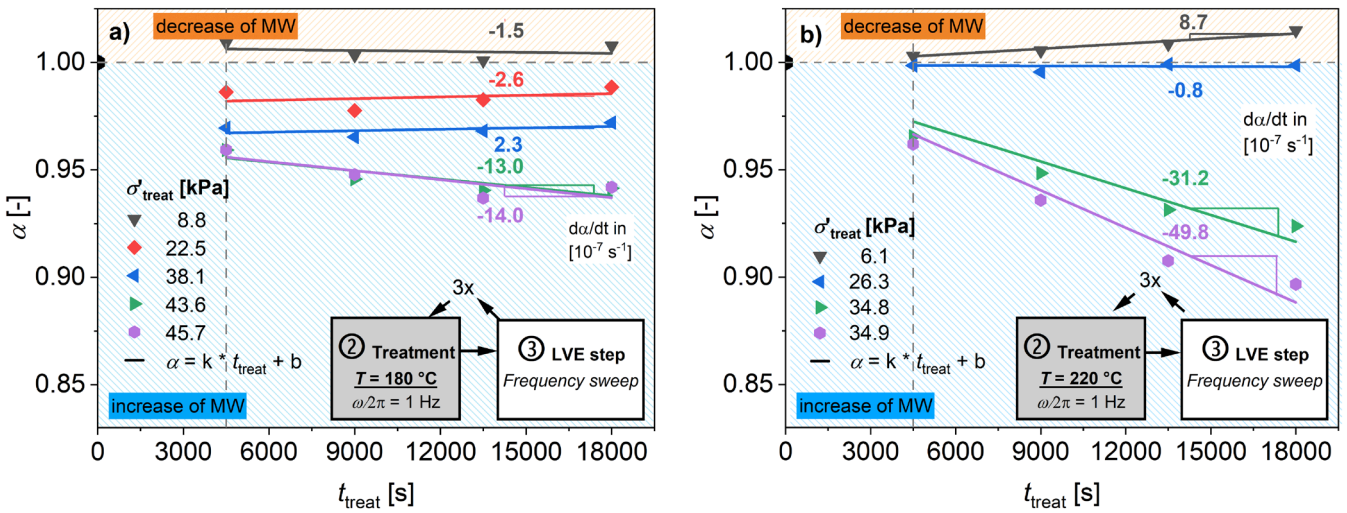

FIGURE 19 | α, indicating the normalized number average molecular weight after treatment, with respect to t_{treat} for different σ'_{treat} at (a) T_{treat} = 180°C and (b) T_{treat} = 220°C. Quasi-stationarity of radical concentration is assumed to be reached for t_{treat} > 75 min. Linear fit was applied to calculate slope $k = d\alpha/dt$ for t_{treat} > 75 min. Further investigated T_{treat} can be found in Figure S5. [Color figure can be viewed at wileyonlinelibrary.com]

up to 18.6%. The VI of the samples treated at T = 160°C show no significant change. Table 7 shows a comparison of the increase in molecular weight and the increase in *VI* from various HDPEs reported in the literature. The data in this article accord with the reported data from literature.

It is also possible to analyze the dominant reaction using the CH_3-absorption with respect to CH_2-absorption [62]. These —CH_3/—CH_2 ratio show a high standard deviation of the investigated integrals of the; therefore, the analysis of this data is vague. The spectral ratios are shown in Figure S4.

With respect to the COI, the HDPE shows an increase no significant change due to the thermo-mechanical treatment with respect to the high standard deviations (Figure 17b). This suggests that oxidation plays no significant role at all used T_{treat}. Table 7 shows a comparison of the change in the *COI* within the literature. As it can be seen, the increase in *COI* in this article is lower than to the shown literature references. This deviation can be explained, because the treatments from the literature references were conducted using a standard extrusion setup. Since this is not a closed system, the HDPE melt is exposed to air at a high temperature that promotes oxidation.

4.4.3 | Isothermal OIT

The OIT was determined for samples treated under conditions shown in Figure 18. The OIT was determined as the crossover of the baseline at the start of the measurement and the tangent

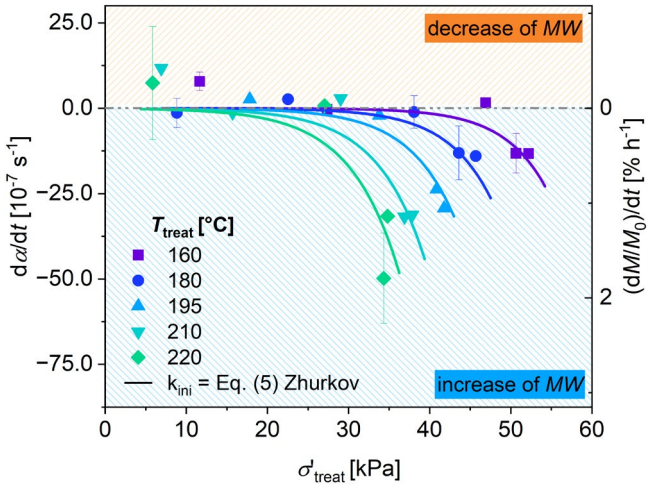

FIGURE 20 | The rate of change in the relative molecular weight as a function of the applied σ'_{treat} during thermo-mechanical treatment. Data are displayed for T_{treat} = 160°C–220°C. Solid lines were fitted by Equation (4). This includes Equation (5) to calculate k_{ini}. [Color figure can be viewed at wileyonlinelibrary.com]

TABLE 8 | Fitting parameters for Equation (4) to calculate k_{ini} to calculate the rate of the change in the relative molecular weight as a function of T_{treat} and σ'_{treat}.

Parameter	Fixed values for fitting	Unit	Lit. reference
k_{rec}	6×10^{9}	L mol^{-1} s^{-1}	[7]
$k_{0,ini}$	1.5×10^{10}	mol L^{-1} s^{-1}	[8]
$k_{0,sc}$	1.5×10^{10}	s^{-1}	[7]
$k_{0,br}$	4.9×10^{8}	L mol^{-1} s^{-1}	[7]
$E_{a,sc}$	66.8	kJ mol^{-1}	[7]
$E_{a,br}$	17.6	kJ mol^{-1}	[7]
β	Free, shared	m^3 mol^{-1}	See Table 9
$E_{a,Ini}$	Free, shared	kJ mol^{-1}	

Note: This includes Equation (5) to calculate the rate of initiation k_{ini}.

TABLE 9 | Results from fitting data by Equation (4) using Equation (5) to calculate the rate of initiation k_{ini}.

β (m^3 mol^{-1})	$E_{a,ini}$ (kJ mol^{-1})	R^2 (-)
1.7	286	0.87

of the exothermic signal of oxidation according to ISO 11357, see Figure 18a.

As shown in Figure 18b, there is a clear decrease in OIT under both T_{treat}. The OIT is significantly lower for samples treated at T_{treat} = 220°C. Additionally, there is no difference between the samples treated at different σ'_{treat}, but at the same T_{treat}. The decrease reaches a plateau of OIT = 2.5 min for t_{treat} > 75 min. The OIT does not change even after longer t_{treat}. This can be explained by the argument that no further reactive antioxidants are left in the sample. Since the samples treated at T_{treat} = 160°C also reach this plateau at t_{treat} = 300 min, it can be concluded that, even after the thermo-mechanical treatment at lowest T_{treat} = 160°C, no active antioxidants are left in the sample.

TABLE 10 | Activation energy of degradation of HDPEs reported in literature measured via TGA and the activation energy for rate of initiation reaction k_{ini} calculated in this article.

Authors	$E_{a,degr}$ (kJ mol^{-1})	Lit. reference
Blaine et al.	190	[67]
van Krevelen et al.	264	[12]
Aboulkas et al.	317	[68]
Klein et al.	206	[69]
This article	$E_{a,ini}$ = 286	

Note: Note that these activation energies describe only the influence of temperature and not of any shear stress.

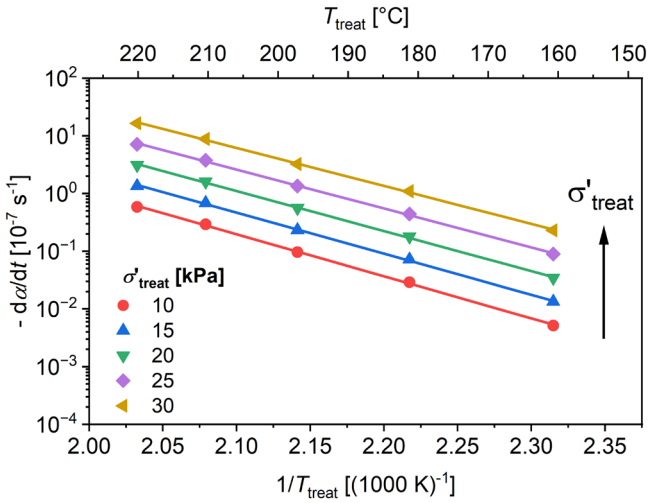

FIGURE 21 | Arrhenius plot of thermo-mechanical treated samples. The points were interpolated from Figure 20 using the fitting results using Equation (5) for the initiation reaction. [Color figure can be viewed at wileyonlinelibrary.com]

4.5 | Reaction Kinetics

To understand the degradation mechanism of the HDPE due to thermo-mechanical treatment, an evaluation of the activation energy for the initiation reaction and the rate of scission and branching is shown in this section. The equations discussed above are applied here.

Figure 15 shows that changes in M_n (number-average molecular weight) and M_w (weight-average molecular weight), due to treatment of the HDPE-samples can be estimated by the scaling law for linear homopolymers $\omega_c^{-1} \propto M^{3.4}$ from rheological data, although there are indications of chain branching of the HDPE [47]. Therefore, the relative molecular weight of the virgin HDPE to the molecular weight after thermo-mechanical treatment, defined as α (Equation 3), is calculated from ω_c by using the following equation:

TABLE 11 | Measured change in α with respect to t_{treat} at different $\omega/2\pi$ and γ_0 than used in this article to validate the suggested model.

ID	$\gamma_{0,treat}$ (%)	$\omega_{treat}/2\pi$ (Hz)	T_{treat} (°C)	σ'_{treat} (kPa)	t_{treat} [min]	$\frac{d\alpha_{measured}}{dt_{treat}}$ (10^{-7} s^{-1})	Standard deviation[a] (10^{-7} s^{-1})	$\frac{d\alpha_{calculated}}{dt_{treat}}$ (10^{-7} s^{-1})
v1	460	2.5	160	65.0	300	−130.4	13.7	−170.3
v2	460	0.4	195	25.7	300	−5.9	13.7	−0.9
v3	460	2.5	195	51.0	300	−95.7	13.7	−124.7
v4	460	0.4	220	21.2	300	−14.7	13.7	−2.5
v5	460	2.5	220	45.2	300	−139.6	13.7	−207.0
v6	630	1	220	31.3	300	−27.3	13.7	−21.3

[a]Standard deviation applied from results with treatment at $T_{treat} = 180$°C and $\sigma'_{treat} = 45.7$ kPa.

$$\alpha(t_{treat}, T_{treat}, \sigma'_{treat}) = \frac{M_0}{M(t_{treat}, T_{treat}, \sigma'_{treat})} = \left(\frac{\omega_c(t_{treat}, T_{treat}, \sigma'_{treat})}{\omega_{c,0}}\right)^{1/3.4} \quad (7)$$

where $\omega_{c,0}$ is the crossover frequency ω_c of the virgin HDPE, and $\omega_c(t_{treat}, T_{treat}, \sigma'_{treat})$ is the ω_c as a function of the treatment conditions.

Figure 19 displays the calculated α, indicating the normalized number average molecular weight after treatment. Due to the assumption of a quasi-stationary level of radicals in the used model (see Equation (4)) and the slow kinetic, a linear change of α for $t_{treat} > 75$ min was assumed. The slopes of this linear change are shown in Figure 19 for $T_{treat} = 180$°C and 220°C. The resulting slopes are shown with respect to σ'_{treat} in Figure 20.

Determining the concentration of double bonds is necessary for the calculation of Equation (4). This was determined by FTIR-measurements. Only the concentration of vinyl groups were calculated, since they have the highest potential to participate in branching [63]. The Beer–Lambert law (Equation 8) was used to estimate the concentration of vinyl groups: [40]

$$c(\text{vinyl}) = \frac{A}{\varepsilon \times d} = \frac{\log(I/I_0)}{\varepsilon \times d} \quad (8)$$

where c is the concentration of vinyl-groups in mol m^{-3}, A is the absorbance of the related group, which is defined as the decadic logarithm of the ratio of the by the medium attenuated intensity to the initial intensity of a light source, d is the thickness of the sample in m and ε is the extinction coefficient in m^3 mol^{-1} m^{-1}. The extinction coefficient of vinyl groups is 12 m^2 mol^{-1} (reported by Haslam et al.) [40] The absorbance of the vinyl groups in the virgin HDPE is 0.035 (unitless) and the thickness of the sample is 70 µm. Using these parameters and Equation (8), a concentration of 0.04 mol L^{-1} of vinyl groups for the virgin HDPE was calculated. This value is within the range reported values in the literature for HDPE (0.007–0.1 mol L^{-1}) [63–66]. These concentrations correspond to a range of 0.09–1.4 vinyl groups per 1000 CH_2-groups.

To fit the data shown in Figure 20 with Equation (4), a least-square fit procedure was performed, where only the free parameters β and $E_{a,ini}$ of Equation (5) were used to calculate the rate of initiation. These parameters were fitted for all applied temperatures simultaneously during the same fitting procedure. All other parameters were fixed to the values shown in Table 8. The results are displayed in Figure 20, and the results for β and $E_{a,Ini}$ are shown in Table 9.

The suggested model describes the measured data with $R^2 = 0.87$. The resulting activation energy is in accordance with activation energy $E_{a,degr}$ of pure thermal degradation using a thermogravimetric analysis (TGA) reported in literature ($E_a = 190$–317 kJ mol^{-1}, see Table 10) [12, 67–69].

The resulting β indicates by its unit an inverse concentration, which is 5×10^{-4} mol L^{-1}. Compared with the concentration of entanglements of the HDPE polymer, which is $c_{entanglements} = 3\,750 \times 10^{-4}$ mol L^{-1} (assuming entanglement molecular weight $M_e = 2$ kg mol^{-1} [70] and density of polymer melt $\rho_{PE} = 0.76$ g cm^{-3} at $T = 180$°C [45]), the concentration calculated from β is smaller by a factor of 1000. Therefore, the origin of the parameter β needs further investigations, but can be a key to gain a better understanding of thermo-mechanical treatment.

An Arrhenius plot can be derived from the results of the fitted curves shown in Figure 20 by interpolating at certain σ'_{treat}. The results are shown in Figure 21.

To validate the suggested model, the variation of further parameters during treatment are used and the results are precalculated using the suggested model and derived parameters (Table 11). The suggested model predicts the results from the different treatment parameters with respect to the standard deviation for the samples that are in the parameter framework of the studied parameters above. The samples treated at higher σ'_{treat} than covered in this article show an overestimation of the calculated $d\alpha/dt$. The validation of the kinetic model is so far restricted to the chosen model HDPE and therefore needs further proofment.

5 | Conclusion

A closed-cavity rheometer (CCR) was used to investigate thermo-mechanical treatment ($\omega/2\pi = 1$ Hz, $\gamma_0 = 28\%$–460%) at temperatures up to $T = 220$°C for up to $t = 300$ min and measure the rheological properties in the linear viscoelastic regime in situ. The

high oscillation amplitudes were chosen to emulate the effect of the shear stress during extrusion and multiple reprocessing of a HDPE. These rheological properties were correlated to physico-chemical changes using HT-SEC and FTIR characterization. These changes can be quantitatively predicted and described by established kinetic models resulting in HDPE-specific kinetic data.

This thermo-mechanical treatment of the studied model HDPE leads to an increase in the molecular weight and branching of the investigated HDPE. Furthermore, higher in-phase shear stress ($>30\,kPa$) leads to stronger increase in molecular weight (up to 13%, determined via HT-SEC and rheology) within the same time. This change is additionally accelerated by higher temperatures.

The HT-SEC results clearly show an increase in molecular weight caused by the applied thermo-mechanical treatment process. The change is in the same order of magnitude as reported in the literature. Results from FTIR analysis show a decrease in the concentration of vinyl bonds due to thermo-mechanical treatment. This may indicate a reaction of macroradicals with these groups, resulting in more branched polymer chains. The flow activation energy increases from $35\,kJ\,mol^{-1}$ by about 16% due to the applied treatment. Thus, it is concluded that branching of the HDPE occurs.

A descriptive model to calculate the resulting molecular weight has been established. For this, the work of Goldberg and Zaikov [7] is combined with the work of Zhurkov [8]. The parameter σ'_{treat} is used to describe the influence of shear stress. The activation energy for the initiation reaction ($=286\,kJ\,mol^{-1}$) and a volume factor ($=1.7\,m^3\,mol^{-1}$) are calculated from this model. This allows thereafter to predict the change in thermo-mechanical treatment. The activation energy is in accordance with data reported from TGA measurements.

As an outlook, it is important to investigate, if the suggested model can be applied to different polyolefins in general, for example, low-density polyethylene (LDPE), linear low-density polyethylene (LLDPE), or isotactic polypropylene (i-PP).

Furthermore, it would be promising to analyze the rheological data during treatment using different rheological methods, for example, FT-rheology or the hyphenated Rheo-IR-setup [71]. This may provide more detailed insights into occurring detailed kinetics. Additionally, it would be interesting to investigate the processing and the crystallization behavior of the thermo-mechanical treated samples to assess the practical relevance of the observed molecular change. It would also be of high interest to elaborate on the suggested model to differentiate between pure chain extension and chain branching.

Author Contributions

Tim Schülein: conceptualization (equal), data curation (lead), formal analysis (lead), investigation (lead), methodology (equal), project administration (lead), resources (lead), software (lead), validation (lead), visualization (lead), writing – original draft (lead), writing – review and editing (equal). **Christos K. Georgantopoulos:** conceptualization (equal), methodology (equal), validation (equal), visualization (equal), writing – review and editing (equal). **Lars Bolk:** formal analysis (supporting), investigation (supporting), writing – review and editing (supporting). **Volker Herrmann:** methodology (equal), project administration (supporting), resources (supporting), supervision (lead), validation (equal), writing – original draft (supporting), writing – review and editing (equal). **Manfred Wilhelm:** formal analysis (supporting), investigation (supporting), methodology (equal), resources (supporting), supervision (lead), validation (equal), visualization (supporting), writing – review and editing (equal).

Acknowledgments

Lyondell-Basell is acknowledged for the donation of the HDPE sample. Prof. Dr. Stefan Mecking is thanked for support for the HT-SEC measurement. We thank Anika Goecke and Micheal Pollard for proofreading of the manuscript. This research did not receive any specific grant from funding agencies in the public, commercial, or not-for-profit sectors. Open Access funding enabled and organized by Projekt DEAL.

Conflicts of Interest

The authors declare no conflicts of interest.

Data Availability Statement

The data that support the findings of this study are available from the corresponding author upon reasonable request.

References

1. European Union: European Commission, "A European Strategy for Plastics in a Circular Economy. COM(2018) 28 Final," 2018.

2. M. K. Loultcheva, M. Proietto, N. Jilov, and F. P. La Mantia, "Recycling of High Density Polyethylene Containers," *Polymer Degradation and Stability* 57 (1997): 77–81.

3. P. Oblak, A. Aulova, M. Bek, and L. S. Per, "The Influence of HDPE Recycling on Rheological Properties and Processing Conditions," *Annual Transactions—Nordic Rheology Society* 26 (2018): 103–107.

4. J. Langwieser, A. Schweighuber, A. Felgel-Farnholz, C. Marschik, W. Buchberger, and J. Fischer, "Determination of the Influence of Multiple Closed Recycling Loops on the Property Profile of Different Polyolefins," *Polymers* 14 (2022): 2429.

5. C. Capone, L. Di Landro, F. Inzoli, M. Penco, and L. Sartore, "Thermal and Mechanical Degradation During Polymer Extrusion Processing," *Polymer Engineering and Science* 2007 (1813): 47.

6. L. A. Pinheiro, M. A. Chinelatto, and S. V. Canevarolo, "The Role of Chain Scission and Chain Branching in High Density Polyethylene During Thermo-Mechanical Degradation," *Polymer Degradation and Stability* 86 (2004): 445–453.

7. V. M. Goldberg and G. E. Zaikov, "Kinetics of Mechanical Degradation in Melts Under Model Conditions and During Processing of Polymers—A Review," *Polymer Degradation and Stability* 19 (1987): 221–250.

8. S. N. Zhurkov and V. E. Korsukov, "Atomic Mechanism of Fracture of Solid Polymers," *Journal of Polymer Science Polymer Physics Edition* 12 (1974): 385–398.

9. K. R. Rajagopal, A. R. Srinivasa, and A. S. Wineman, "On the Shear and Bending of a Degrading Polymer Beam," *International Journal of Plasticity* 23 (2007): 1618–1636.

10. R. S. Porter and A. Casale, "Recent Studies of Polymer Reactions Caused by Stress," *Polymer Engineering and Science* 25 (1985): 129–156.

11. E. G. Eldarov, F. V. Mamedov, V. M. Goldberg, and G. E. Zaikov, "A Kinetic Model of Polymer Degradation During Extrusion," *Polymer Degradation and Stability* 51 (1996): 271–279.

12. D. W. Krevelen and K. te Nijenhuis, *Properties of Polymers: Their Correlation With Chemical Structure Their Numerical Estimation and*

Prediction From Additive Group Contributions, 4th ed. (Amsterdam, Netherlands: Elsevier, 2009).

13. Z. O. G. Schyns and M. P. Shaver, "Mechanical Recycling of Packaging Plastics: A Review," *Macromolecular Rapid Communications* 42 (2021): 2000415.

14. K. D. T. Sánchez, N. S. Allen, C. M. Liauw, and B. Johnson, "Effects of Type of Polymerization Catalyst System on the Degradation of Polyethylenes in the Melt State. Part 1: Unstabilized Polyethylenes (Including Metallocene Types)," *Journal of Vinyl & Additive Technology* 17 (2011): 28.

15. G. R. Rideal and J. C. Padget, "The Thermal-Mechanical Degradation of High Density Polyethylene," *Journal of Polymer Science Polymer Symposium* 57 (1976): 1–15.

16. S. Moss and H. Zweifel, "Degradation and Stabilization of High Density Polyethylene During Multiple Extrusions," *Polymer Degradation and Stability* 25 (1989): 217–245.

17. P. Oblak, J. Gonzalez-Gutierrez, B. Zupančič, A. Aulova, and I. Emri, "Processability and Mechanical Properties of Extensively Recycled High Density Polyethylene," *Polymer Degradation and Stability* 114 (2015): 133–145.

18. S. Apone, R. Bongiovanni, M. Braglia, D. Scalia, and A. Priola, "Effects of Thermomechanical Treatments on HDPE Used for TLC Ducts," *Polymer Testing* 22 (2003): 275–280.

19. T. Kealy, "Rheological Analysis of the Degradation of HDPE During Consecutive Processing Steps and for Different Processing Conditions," *Journal of Applied Polymer Science* 112 (2009): 639–648.

20. J. Zhang, V. Hirschberg, A. Goecke, et al., "Effect of Mechanical Recycling on Molecular Structure and Rheological Properties of High-Density Polyethylene (HDPE)," *Polymer* 297 (2024): 126866.

21. M. H. Akhras, J. Langwieser, S. Czaker, A. Felgel-Farnholz, and J. Fischer, "Cascadic Degradation of Selected Polyolefin Grades in a Simulated Closed-Loop Recycling Process," *Clean Technologies and Environmental Policy* 26 (2024): 3507–3526.

22. J. Dostál, V. Kašpárková, M. Zatloukal, J. Muras, and L. Šimek, "Influence of the Repeated Extrusion on the Degradation of Polyethylene. Structural Changes in Low Density Polyethylene," *European Polymer Journal* 44 (2008): 2652–2658.

23. H. Jin, J. Gonzalez-Gutierrez, P. Oblak, B. Zupančič, and I. Emri, "The Effect of Extensive Mechanical Recycling on the Properties of Low Density Polyethylene," *Polymer Degradation and Stability* 97 (2012): 2262–2272.

24. S. Al-Malaika, U. Daraz, and S. Issenhuth, "Effect of Processing Conditions and Catalyst Type on the Thermal Oxidative Degradation Mechanisms and Melt Stability of Metallocene and Ziegler-Catalyzed Ethylene-1-Hexene Copolymers," *Journal of Vinyl & Additive Technology* 28 (2022): 254–273.

25. L. A. Pinheiro, M. A. Chinelatto, and S. V. Canevarolo, "Evaluation of Philips and Ziegler–Natta High-Density Polyethylene Degradation During Processing in an Internal Mixer Using the Chain Scission and Branching Distribution Function Analysis," *Polymer Degradation and Stability* 91 (2006): 2324–2332.

26. E. M. Hoàng, N. S. Allen, C. M. Liauw, E. Fontán, and P. Lafuente, "The Thermo-Oxidative Degradation of Metallocene Polyethylenes: Part 2: Thermal Oxidation in the Melt State," *Polymer Degradation and Stability* 91 (2006): 1363–1372.

27. A. Schweighuber, A. Felgel-Farnholz, T. Bögl, J. Fischer, and W. Buchberger, "Investigations on the Influence of Multiple Extrusion on the Degradation of Polyolefins," *Polymer Degradation and Stability* 192 (2021): 109689.

28. S. Littek, M. Schneider, K. Huber, and V. Schöppner, "Messung zum Materialabbau von Polypropylen," *Kunststofftechnik* 8 (2012): 416–428.

29. C. Schall and V. Schöppner, "Measurement of Material Degradation in Dependence of Shear Rate, Temperature, and Residence Time," *Polymer Engineering and Science* 62 (2022): 815–823.

30. S. G. Tikhomirov, S. L. Podvalny, A. A. Khvostov, O. V. Karmanova, and V. K. Bityukov, "Study and Modeling of Polymer Degradation in Bulk," *Theoretical Foundations of Chemical Engineering* 52 (2018): 78–86.

31. H. Kaneyasu, P. Phanthong, H. Okubo, and S. Yao, "Investigation of Degradation Mechanism From Shear Deformation and the Relationship With Mechanical Properties, Lamellar Size, and Morphology of High-Density Polyethylene," *Applied Sciences* 11 (2021): 8436.

32. H. Münstedt, "Rheological Measurements and Structural Analysis of Polymeric Materials," *Polymers* 13 (2021): 1123.

33. D. Auhl, J. Stange, H. Münstedt, et al., "Long-Chain Branched Polypropylenes by Electron Beam Irradiation and Their Rheological Properties," *Macromolecules* 37 (2004): 9465–9472.

34. C. Gabriel, J. Kaschta, and H. Münstedt, "Comparison of Different Shear Rheometers With Regard to Creep and Creep Recovery Measurements," *Rheologica Acta* 37 (1998): 358–364.

35. F. Ellwanger, C. K. Georgantopoulos, H. P. Karbstein, M. Wilhelm, and M. Azad Emin, "Application of the Ramp Test From a Closed Cavity Rheometer to Obtain the Steady-State Shear Viscosity $\eta(\dot{\gamma})$," *Applied Rheology* 33 (2023): 20220149.

36. M. A. Cziep, M. Abbasi, M. Heck, L. Arens, and M. Wilhelm, "Effect of Molecular Weight, Polydispersity, and Monomer of Linear Homopolymer Melts on the Intrinsic Mechanical Nonlinearity 3 Q 0 (ω) in MAOS," *Macromolecules* 49 (2016): 3566–3579.

37. B. Debbaut and H. Burhin, "Large Amplitude Oscillatory Shear and Fourier-Transform Rheology for a High-Density Polyethylene: Experiments and Numerical Simulation," *Journal of Rheology* 46 (2002): 1155–1176.

38. H. G. Burhin, T. Rauschmann, and H.-J. Graf, "New and Highly Efficient Method to Measure Steady Shear Viscosity and Wall Slip of Rubber Compounds: Closed-Boundary Rheometer (RPA)," *Rubber Chemistry and Technology* 95 (2022): 413–424.

39. C. Rauwendaal and P. J. Gramann, *Polymer Extrusion*, 5th ed. (Munich: Hanser, 2014).

40. J. Haslam, H. A. Willis, and D. C. M. Squirrel, *Identification and Analysis of Plastics*, 2nd ed. (New York: Wiley Heyden Ltd, 1983).

41. G. Grause, M.-F. Chien, and C. Inoue, "Changes During the Weathering of Polyolefins," *Polymer Degradation and Stability* 181 (2020): 109364.

42. L. C. Mendes, E. S. Rufino, F. O. C. de Paula, and A. C. Torres, Jr., "Mechanical, Thermal and Microstructure Evaluation of HDPE After Weathering in Rio de Janeiro City," *Polymer Degradation and Stability* 79 (2003): 371–383.

43. J. Almond, P. Sugumaar, M. N. Wenzel, G. Hill, and C. Wallis, "Determination of the Carbonyl Index of Polyethylene and Polypropylene Using Specified Area Under Band Methodology With ATR-FTIR Spectroscopy," *e-Polymers* 20 (2020): 369–381.

44. M. Sudhakar, A. Trishul, M. Doble, et al., "Biofouling and Biodegradation of Polyolefins in Ocean Waters," *Polymer Degradation and Stability* 92 (2007): 1743–1752.

45. A. Rudin and R.-J. Chang, "A Study of Melt Density of Flowing Linear Polyethylene," *Journal of Applied Polymer Science* 22 (1978): 781–799.

46. I. B. Kazatchkov, S. G. Hatzikiriakos, N. Bohnet, and S. K. Goyal, "Influence of Molecular Structure on the Rheological and Processing Behavior of Polyethylene Resins," *Polymer Engineering and Science* 39 (1999): 804–815.

47. I. Vittorias, D. Lilge, V. Baroso, and M. Wilhelm, "Linear and Non-Linear Rheology of Linear Polydisperse Polyethylene," *Rheologica Acta* 50 (2011): 691–700.

48. E. Mitsoulis and S. G. Hatzikiriakos, "Rheological Properties Related to Extrusion of Polyolefins," *Polymers* 13 (2021): 489.

49. C. Liu, J. He, E. van Ruymbeke, R. Keunings, and C. Bailly, "Evaluation of Different Methods for the Determination of the Plateau Modulus and the Entanglement Molecular Weight," *Polymer* 47 (2006): 4461–4479.

50. S. Trinkle and C. Friedrich, "Van Gurp-Palmen-Plot: A Way to Characterize Polydispersity of Linear Polymers," *Rheologica Acta* 40 (2001): 322–328.

51. S. Trinkle, P. Walter, and C. Friedrich, "Van Gurp-Palmen Plot II–Classification of Long Chain Branched Polymers by Their Topology," *Rheologica Acta* 41 (2002): 103–113.

52. Y. Yu, P. J. DesLauriers, and D. C. Rohlfing, "SEC-MALS Method for the Determination of Long-Chain Branching and Long-Chain Branching Distribution in Polyethylene," *Polymer* 46 (2005): 5165–5182.

53. M. van Gurp and J. Palmen, "Time-Temperature Superposition for Polymeric Blends," *Rheology Bulletin* 67 (1998): 5.

54. P. Wood-Adams and S. Costeux, "Thermorheological Behavior of Polyethylene: Effects of Microstructure and Long Chain Branching," *Macromolecules* 34 (2001): 6281–6290.

55. B. H. Bersted, "On the Effects of Very Low Levels of Long Chain Branching on Rheological Behavior in Polyethylene," *Journal of Applied Polymer Science* 30 (1985): 3751–3765.

56. J. F. Vega, A. Santamaría, A. Muñoz-Escalona, and P. Lafuente, "Small-Amplitude Oscillatory Shear Flow Measurements as a Tool to Detect Very Low Amounts of Long Chain Branching in Polyethylenes," *Macromolecules* 31 (1998): 3639–3647.

57. F. J. Stadler, J. Kaschta, and H. Münstedt, "Thermorheological Behavior of Various Long-Chain Branched Polyethylenes," *Macromolecules* 41 (2008): 1328–1333.

58. D. Ahirwal, S. Filipe, I. Neuhaus, M. Busch, G. Schlatter, and M. Wilhelm, "Large Amplitude Oscillatory Shear and Uniaxial Extensional Rheology of Blends From Linear and Long-Chain Branched Polyethylene and Polypropylene," *Journal of Rheology* 58 (2014): 635–658.

59. H. Münstedt, "The Influence of Various Deformation Histories on Elongational Properties of Low Density Polyethylene," *Colloid & Polymer Science* 259 (1981): 966–972.

60. M. Rokudai and T. Fujiki, "Influence of Shearing History on the Rheological Properties and Processability of Branched Polymers. III. An Amorphous Long-Chain Branched Polymer," *Journal of Applied Polymer Science* 23 (1979): 3295–3300.

61. K. Klimke, M. Parkinson, C. Piel, W. Kaminsky, H. W. Spiess, and M. Wilhelm, "Optimisation and Application of Polyolefin Branch Quantification by Melt-State ^{13}C NMR Spectroscopy," *Macromolecular Chemistry and Physics* 207 (2006): 382–395.

62. C. Baker and W. F. Maddams, "Infrared Spectroscopic Studies on Polyethylene, 1. The Measurement of Low Levels of Chain Branching," *Makromolekulare Chemie* 177 (1976): 437–448.

63. R. L. Clough, N. C. Billingham, and K. T. Gillen, *Polymer Durability: Degradation, Stabilization, and Lifetime Prediction*, vol. 249 (Washington, DC: American Chemical Society, 1996), 651.

64. M. Dole, D. C. Milner, and T. F. Williams, "Irradiation of Polyethylene. II. Kinetics of Unsaturation Effects," *Journal of the American Chemical Society* 80 (1958): 1580.

65. M. N. Pedernera, C. Sarmoria, E. M. Vallés, and A. Brandolin, "An Improved Kinetic Model for the Peroxide Initiated Modification of Polyethylene," *Polymer Engineering and Science* 39 (1999): 2085–2095.

66. A. Brandolin, C. Sarmoria, M. D. Failla, and E. M. Vallés, "Mathematical Modeling of the Reactive Modification of High-Density Polyethylene. Effect of Vinyl Content," *Industrial and Engineering Chemistry Research* 46 (2007): 7561–7570.

67. R. L. Blaine and B. K. Hahn, "Obtaining Kinetic Parameters by Modulated Thermogravimetry," *Journal of Thermal Analysis* 54 (1998): 695–704.

68. A. Aboulkas, K. El Harfi, and A. El Bouadili, "Thermal Degradation Behaviors of Polyethylene and Polypropylene. Part I: Pyrolysis Kinetics and Mechanisms," *Energy Conversion and Management* 51 (2010): 1363–1369.

69. J. M. Klein, G. R. Ramos, A. M. C. Grisa, R. N. Brandalise, and M. Zeni, "Thermogravimetric and Morphologic Analysis of Oxo-Degradable Polyethylene Films After Accelerated Weathering," *Progress in Rubber, Plastics and Recycling Technology* 29 (2013): 39–54.

70. V. M. Litvinov, M. E. Ries, T. W. Baughman, A. Henke, and P. P. Matloka, "Chain Entanglements in Polyethylene Melts. Why Is It Studied Again?," *Macromolecules* 46 (2013): 541–547.

71. N. W. Radebe, C. Fengler, C. O. Klein, R. Figuli, and M. Wilhelm, "Rheo-IR: A Combined Setup for Correlating Chemical Changes via FTIR Spectroscopy and Rheological Properties in a Strain-Controlled Rheometer," *Journal of Rheology* 65 (2021): 681–693.

Supporting Information

Additional supporting information can be found online in the Supporting Information section.